Spring 5-2002

Precision Electrolytic Nanofabrication

Kent Cooksey Wilcher
University of Tennessee - Knoxville

Precision Electrolytic Nanofabrication

Kent Wilcher

Senior Honors Project

The University of Tennessee, Knoxville

Oak Ridge National Laboratory

Knoxville, TN 37919

Submitted: May 03, 2002

Table of Contents

Abstract	iii
Introduction	1
Methods and Materials	2
Results	4
Discussion and Conclusions	8
Acknowledgments	9
References	10
Figures	11
Tables	21

Abstract

The ability to manipulate individual molecules is of fundamental importance in the development of the next generation of nanoscale devices. One of the major difficulties encountered in the fabrication of such devices is the creation of the interface between macroscopic structures and individual molecules. This project involved the fabrication of nanoelectrodes by precise electrolytic deposition of metal onto a substrate. The substrate consisted of two gold electrodes separated by a distance of approximately one micron, fabricated using electron beam lithography. Metal was then deposited on the tip of one of the electrodes by applying a potential across the gap using a programmable pulse current source while under an electrolytic solution containing metal compounds. The focused electric field generated across the gap between the two electrodes theoretically allows for deposition of metal only at the tip of the negative electrode. The amount and location of the deposition was monitored *in situ* using an Atomic Force Microscope (AFM). The goal of this project was to demonstrate the ability to create a nanometer-scale gap suitable for molecular applications.

Category: Chemical Engineering
School Author Attends: University of Tennessee, Knoxville
DOE National Laboratory: Oak Ridge National Laboratory
Mentor's Name: James W. Lee

Presenter's Name: Kent Wilcher
Mailing Address: 7134 Deane Hill
City/State/Zip: Knoxville, TN 37919
Phone: 865-560-0389
Email Address: kwilcher@utk.edu

Introduction

The goal of this project was to develop a repeatable and precisely controlled method to create electrodes with molecular scale (1-10 nanometers) distance between terminals. Even with the most precise lithographic techniques it is very difficult, expensive, and time consuming to produce electrodes separated by distances of less around 25 nm[1]. This type of device is expected to be useful primarily because it provides new opportunities and abilities to manipulate and measure single molecules, nanoparticles, and possibly even atoms. The basic techniques used to fabricate these electrodes (electron-beam lithography and electrochemical deposition) are well suited to large scale fabrication processes, suggesting that such electrodes could be produced in bulk quantities and used to aid in a variety of nanoscale experiments and devices.

Methods and Materials

The initial structure was constructed using electron beam lithography to create gold electrodes on a silicon oxide substrate. The gold was deposited in the shape of large gold contact pads connected to the smaller microelectrodes. The electrodes and gold pads were constructed by depositing 10 nanometers of titanium followed by 40 nanometers of gold onto the silicon oxide surface using chemical vapor deposition. Initially the microelectrodes were approximately 50 microns long and 1.5 microns wide, with a distance of 1 micron between the tips of the electrodes. Conductive silver adhesive was used to connect wires to the gold contact pads. The device was then mounted on an AFM puck using torr sealant. Figure 1 depicts the basic structure and scale of the microelectrodes before any deposition was attempted.

Initially 100 mL solutions of 10 mM $Ni(II)Cl_2$, 10mM $Pt(NH_3)_4Cl_2$, 10 mM $Co(II)Cl_2$, 10mM $Cu(II)Cl_2$, and 10mM $KAu(CN)_2$ were prepared, with the $KAu(CN)_2$ also containing 1M $KHCO_3$ and 0.2 M KOH to buffer the solution to a basic pH (approximately 10). The 10 mM $Ni(II)Cl_2$ solution was later buffered to basic pH also. Deposition was accomplished by using an HP-72J programmable voltage source to apply a potential across the gap between the electrodes while the device was under one of the above electrolyte solutions. During the deposition reaction the metal ion accepts an electron from the negative electrode and forms a neutral, stable metal atom on the surface of the electrode. For

deposition a negative potential was applied at one electrode with the other electrode being set up as ground. Although the focus for this experiment was deposition, it is obviously possible to deplete the electrodes by applying a positive potential across the gap in a suitable solution. A digital oscilloscope and counter were used to monitor the output from the pulse generator and ensure that it was functioning properly and as programmed. A Digital Instruments multimode AFM, operating in contact mode, was used in concert with a liquid cell sample holder to monitor the electrodes during deposition.

Results and Discussion

Initially the deposition of gold, platinum, nickel, and cobalt was verified using the 10 mM solutions described earlier and potentials of approximately –1.0 to –1.5 V, with pulse durations of 100-300 microseconds and pulse frequencies on the order of 3 kHz. The results obtained using nickel, of interest because of its use as a catalyst for nanotube growth, are of particular interest and are discussed in greater detail later on. While initial deposition attempts were successful in depositing metal onto the negative electrode, the deposition occurred all along the electrode in a nearly equal amount, as opposed to the desired goal of depositing only on the tip of the electrode axially towards the opposing (ground) electrode. An example of this type of deposition is given in figure 2. Several possible reasons for this were explored.

First was the possibility that the connection between the macrostructure and microelectrodes was not complete for one of the electrodes. If, for instance, the circuit between the negative wire and negative electrode was not connected all the way out to the tip of the electrode the electric field generated by the voltage source would extend from the area of the disconnect to the ground electrode. Ideally this electric field should extend axially from the tip of one electrode to the tip of another. It was found to be possible to measure the impedance of the connection between the connecting wire and the macrostructure directly beside the microelectrode using a multimeter and a small wire. Using this measurement it was then possible to determine whether or not

the bulk connection was faulty, with an impedance (including some contact loss due to poor measuring wire connection) of between 5-150 ohms expected for an intact half-circuit (from one wire to a corresponding gold pad right before the microelectrode). Inspection with the AFM could then be used to verify that the actual microelectrode structure was intact and not suffering from a gross defect (see Figure 3). Using these techniques several macro-structural defects created during initial fabrication or during post-lithographic handling were found, and, when possible, repaired with a conductive silver liquid.

Although inspecting the macro- and micro- structures carefully for defect helped to insure that no gross connection failure was causing irregular deposition, even structures verified to be intact in every way still exhibited deposition all along the electrode, although usually in greater amount at the tip of the electrode. One possible explanation for this behavior was that deposition of material at the gap quickly depleted the surrounding solution of metal ions, resulting in a deficit of ions in the vicinity of the gap. Therefore deposition all along the electrode could occur in order to equalize the charge building up on it. To account for this effect pulse times were shortened to 5-20 microseconds and pulse frequencies moved to 500-1000 Hz. As seen in Figures 4 and 5 these modifications resulted in deposition occurring primarily at the tip of the electrode but still also somewhat on the sides and top of the electrode. In addition to this problem, it was also noticed that as many consecutive experiments were performed with the $NiCl_2$ solution the ground electrode was being depleted (see Tables 1 and 2 and Figures 6, 7, and 8).

One possible explanation is that the voltage source was not perfectly grounded. Even a slightly positive potential occurring at the 'ground' terminal could have, over a long period of time (in comparison with the very short time-frame for negative potential application), caused gradual depletion of the ground electrode. This was easily corrected by simply grounding the voltage generator's 'ground' terminal to a true earth ground. One consequence of this depletion is that as experiments were performed to determine the optimum settings for the voltage source to maximize the precision of the deposition the ground electrode was being slowly depleted, changing the characteristics of the electric field between the two electrodes. Experiments to verify that this depletion problem has been solved by grounding the voltage source are still ongoing.

When the 10 mM $NiCl_2$ solution was used to deposit nickel onto an electrode it was observed that almost immediately the deposited nickel was reabsorbed into solution. Figures 9 and 10 demonstrate this process. Typically within 30 seconds of the deposition of a similar amount as in Figure 9 all Ni would have dissolved away, leaving the electrode in essentially the same condition it was in pre-deposition. It was determined that the cause of this solid Ni instability in solution was due to the slightly acidic pH (about 6.85) of the solution. By changing the pH to approximately 9.9 using a buffer solution it was possible to get the Ni to remain stable after deposited on an electrode. Despite the eventual undesirability of having unstable nickel, it proved extremely useful experimentally because it allowed one to test voltage source settings or solution

concentrations repeatable using the same expensive-to-fabricate electrode structure.

Conclusion

The deposition process definitely functions with a variety of metal ions, and can be shown to be fairly selectively on the tip of the electrodes, but the desired precision deposition on the tip of the electrode *only* has not been demonstrated so far. Some problems with the deposition setup and process have been found and presumadely corrected but further experimentation is needed to insure that with an intact and functional macrostructure, adequate time given for diffusion to occur between pulses, and grounding problems solved that reproducible deposition occurs only axially out from the tip of the negative electrode, not on the sides that has occurred previously. Having shown that it is possible to deposit nickel, and, by modifying the pH of the solution make the nickel remain on the electrode, if precise deposition on the tip of the electrode could be achieved these electrodes could be used for one of the many potential applications for nanoelectrodes, nanotube growth.

Acknowledgements

I would like to thank my mentor, Dr. James W. Lee, for giving me the opportunity to work on and learn from such an interesting project. Also special thanks go to Dr. Ida Lee and Dr. Thomas Thundat for providing valuable advice and expertise regarding AFM operation.

Thanks also go to the Department of Energy funded ERULF and ORISE programs, without which none of this would have been possible.

References

[1]Lee, J. W., and Greenbaum, E. Patent Application, 1999, No. 0772.1: Programmable Nanometer-Scale Electrolytic Deposition and Depletion.

Figures

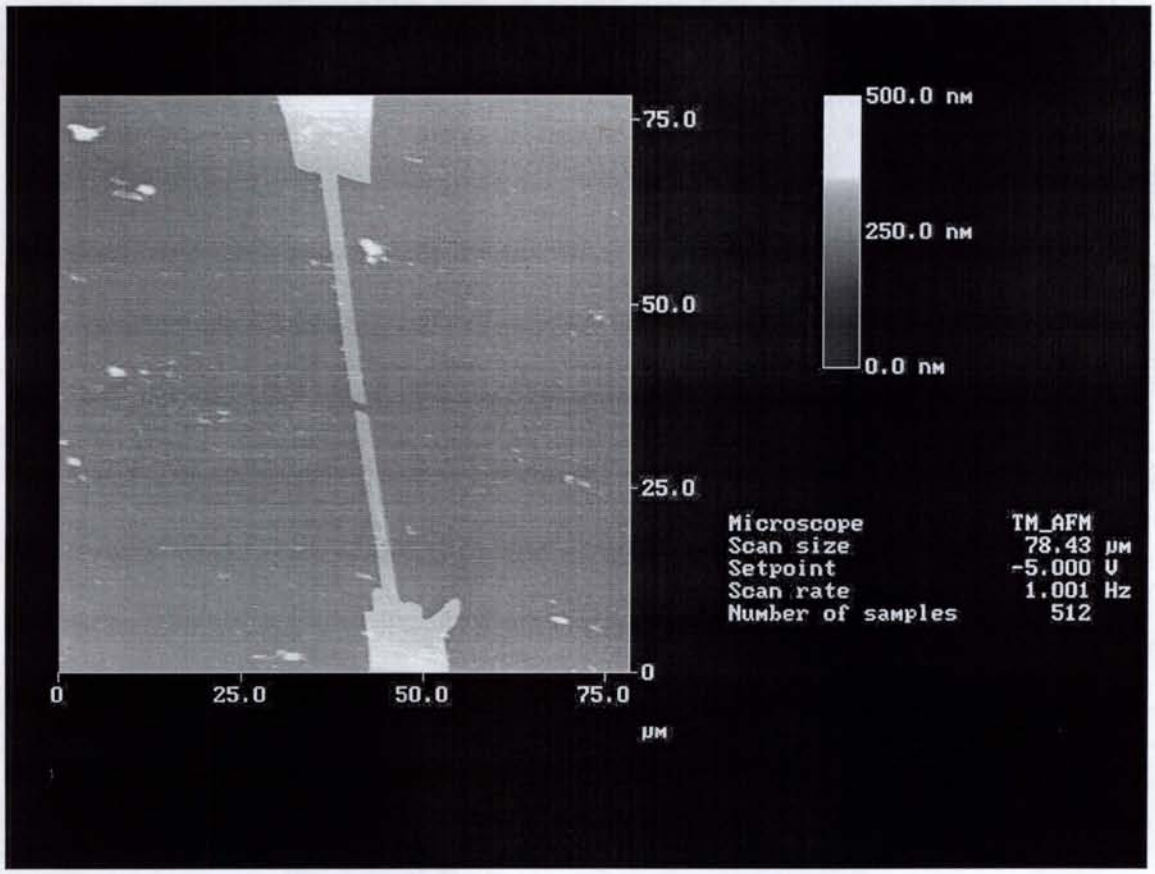

Figure 1: Overall geometry of the microelectrodes and connecting gold structure

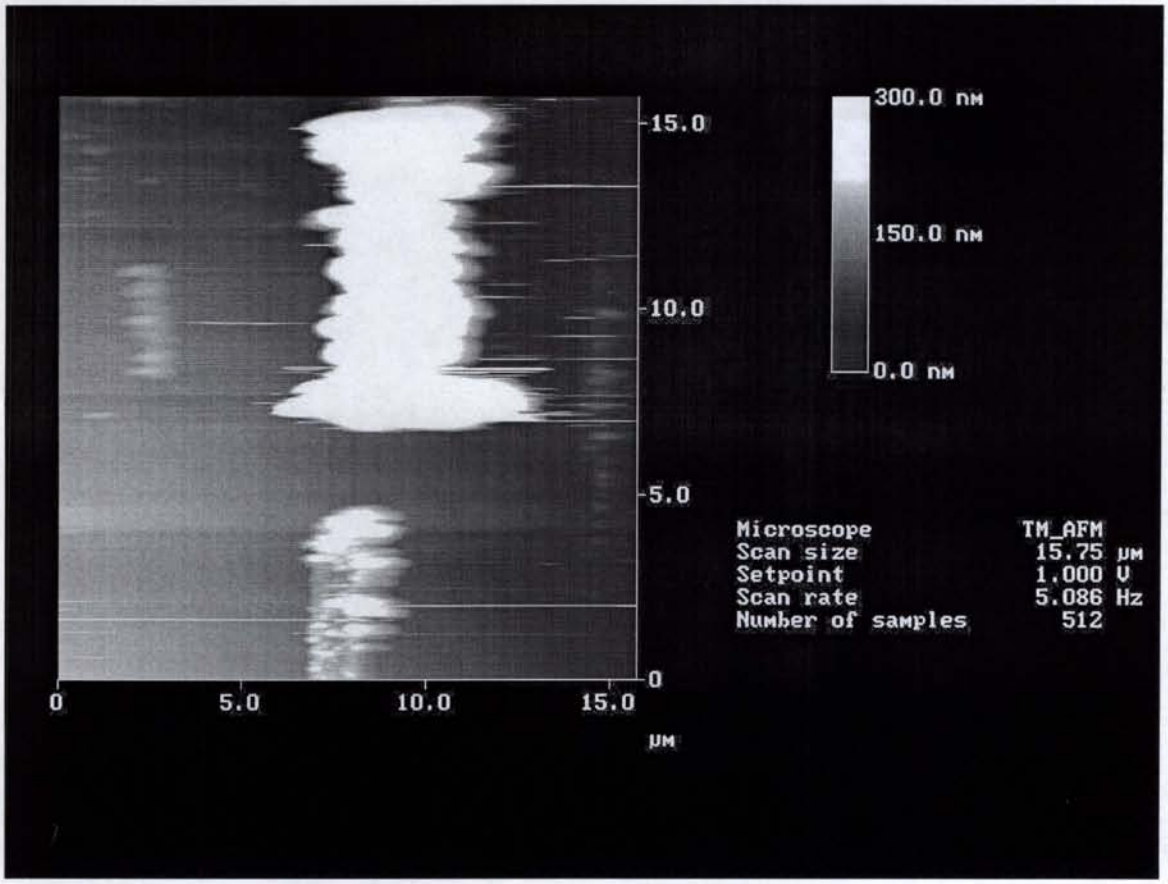

Figure 2: Initial Deposition Attempt (using 10 mM $Pt(NH_3)_4Cl_2$)

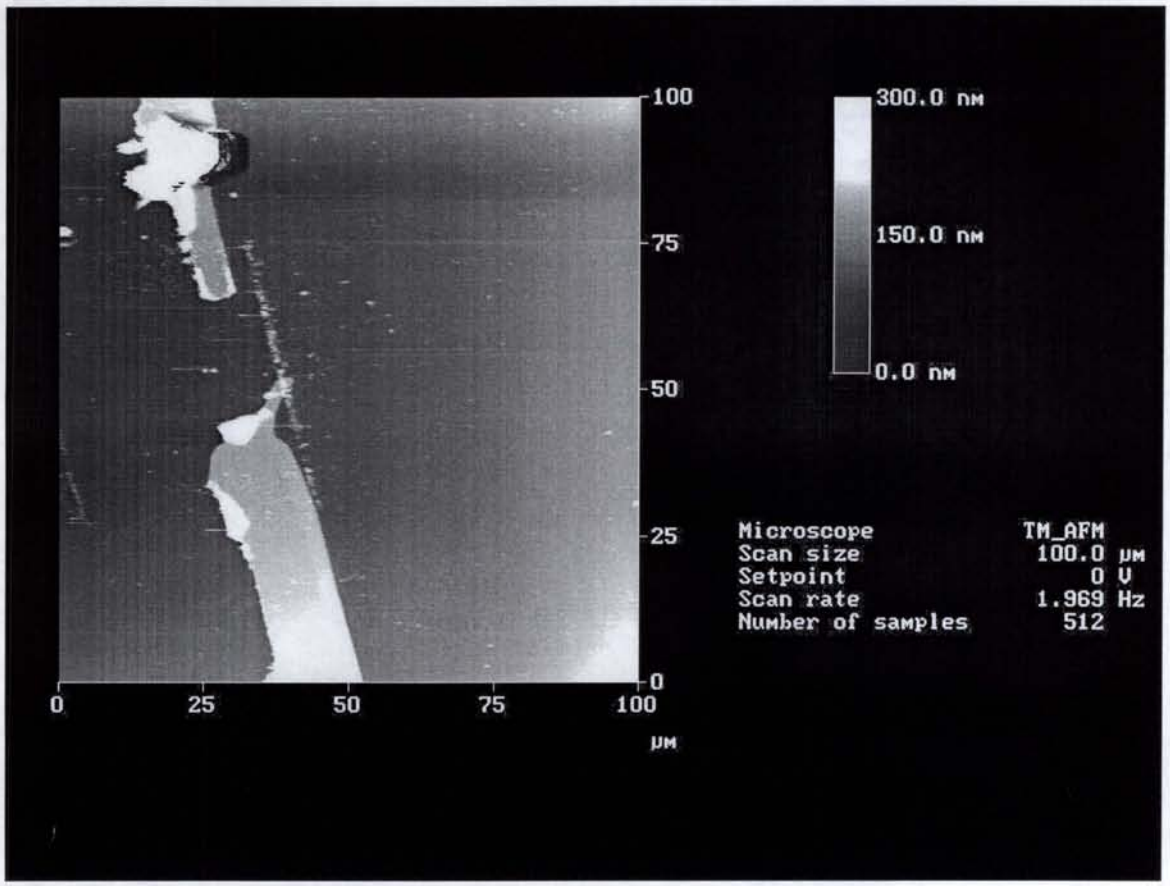

Figure 3: Defective microelectrode. Gap approximately 20 microns across

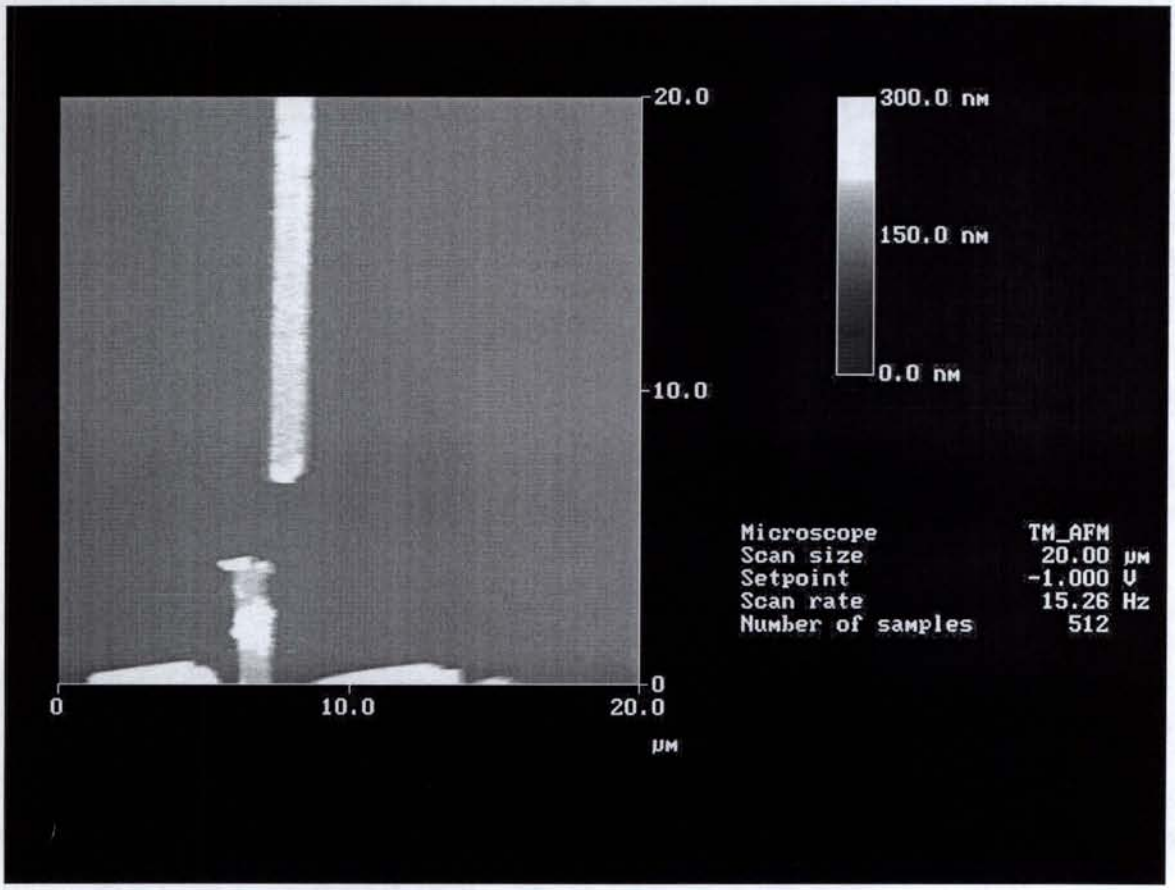

Figure 4: Pre-deposition condition of device #6

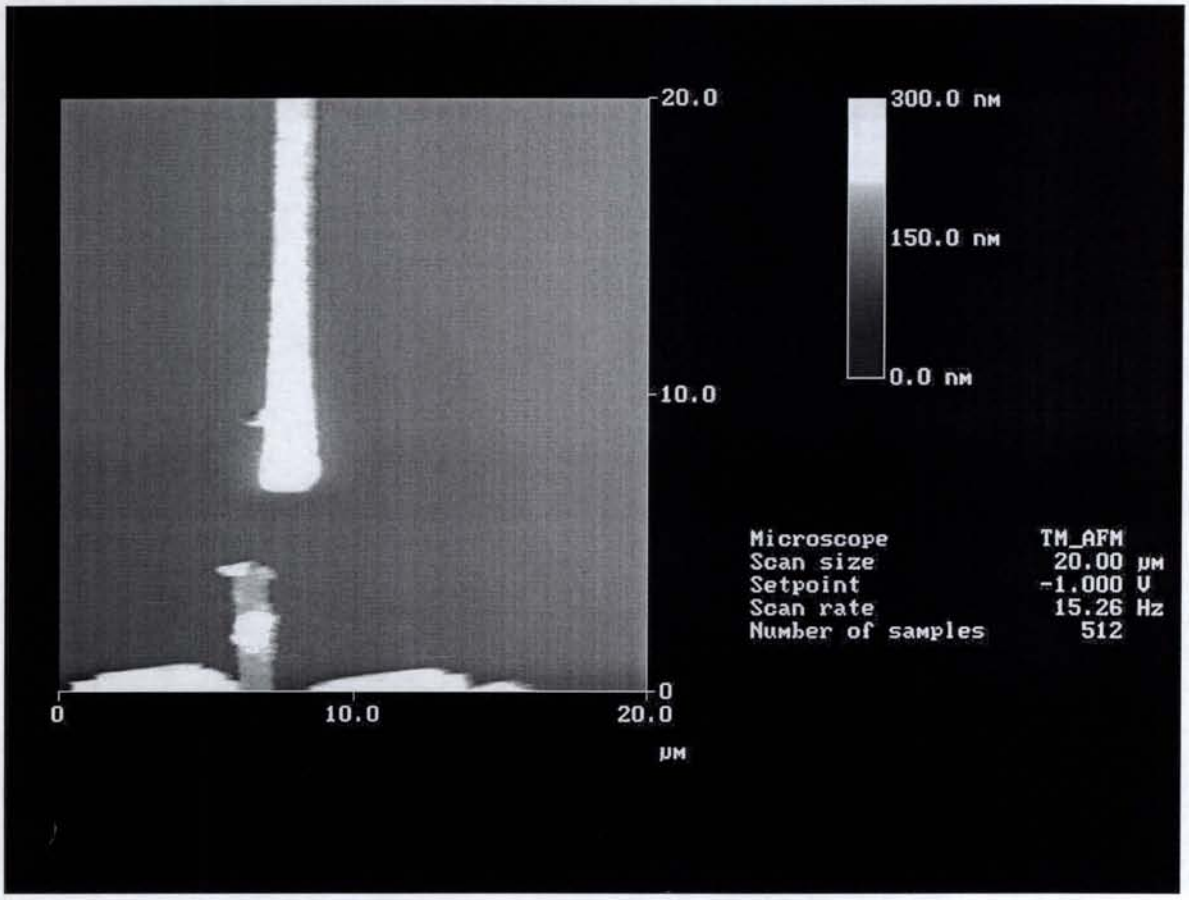

Figure 5: Deposition of Ni in 10 mM $NiCl_2$ using 1500 20 microsecond pulses at 1 KHz (Device #6)

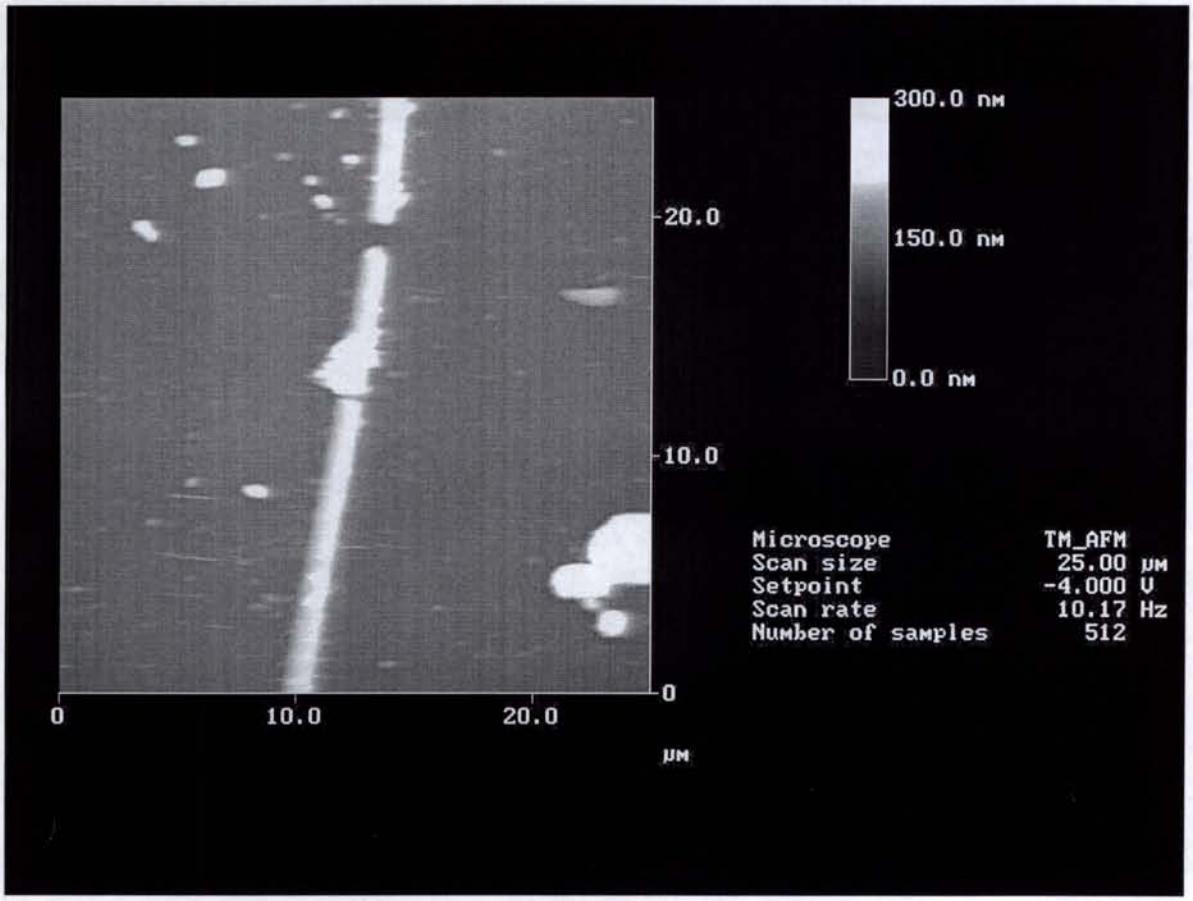

Figure 6: Pre-experiment condition of device #4

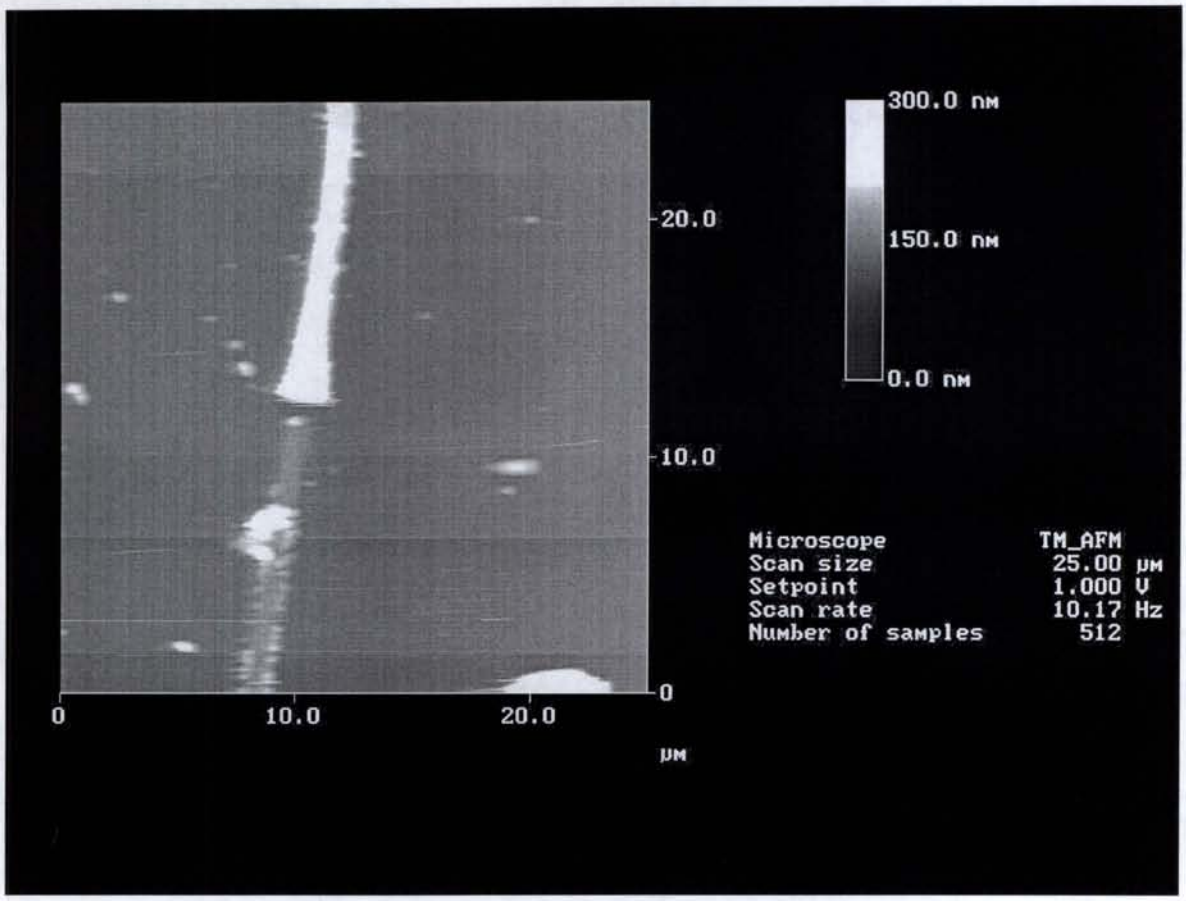

Figure 7: Condition of device #4 after multiple deposition and dissolution of Ni (top electrode negative, bottom electrode ground)

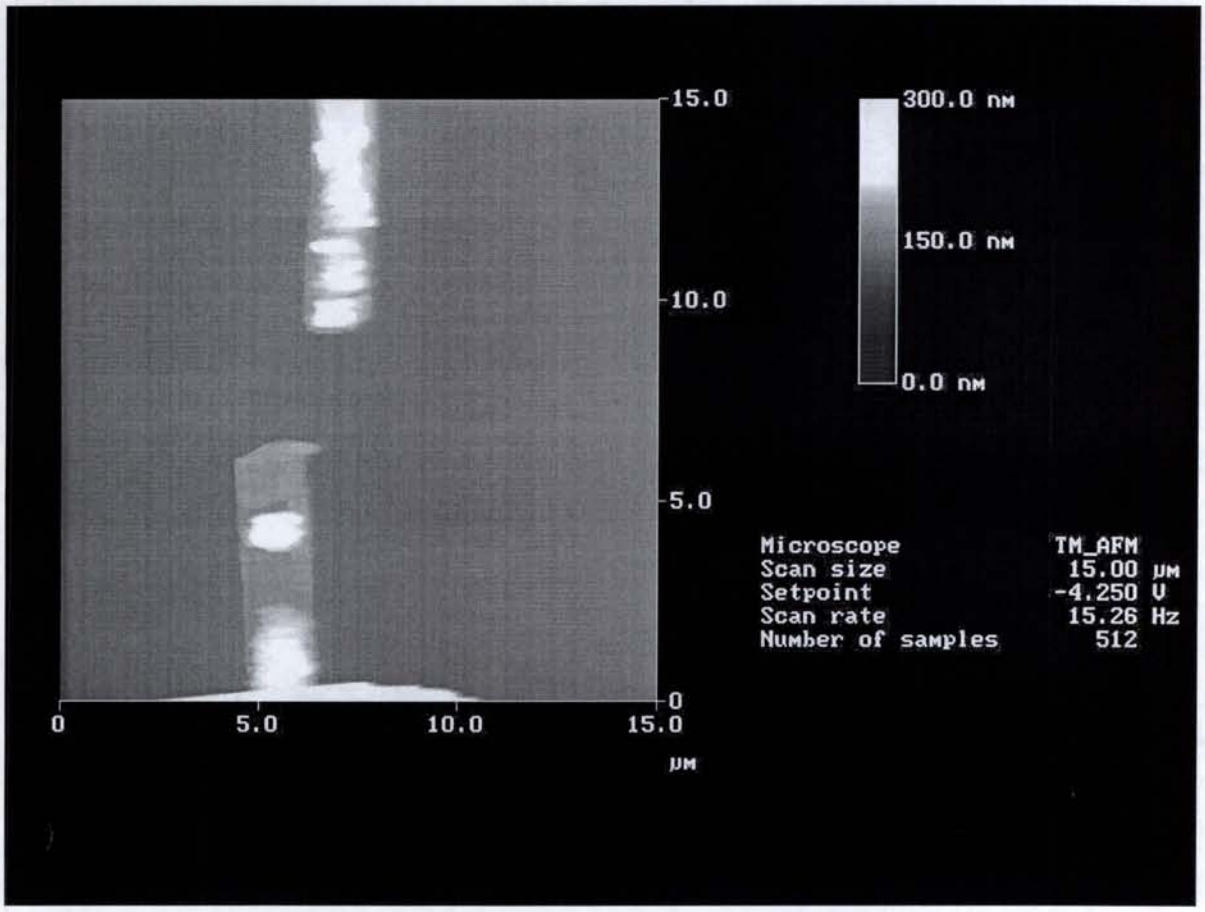

Figure 8: Condition of device #6 after multiple deposition and dissolution of Ni (top electrode negative, bottom electrode positive)

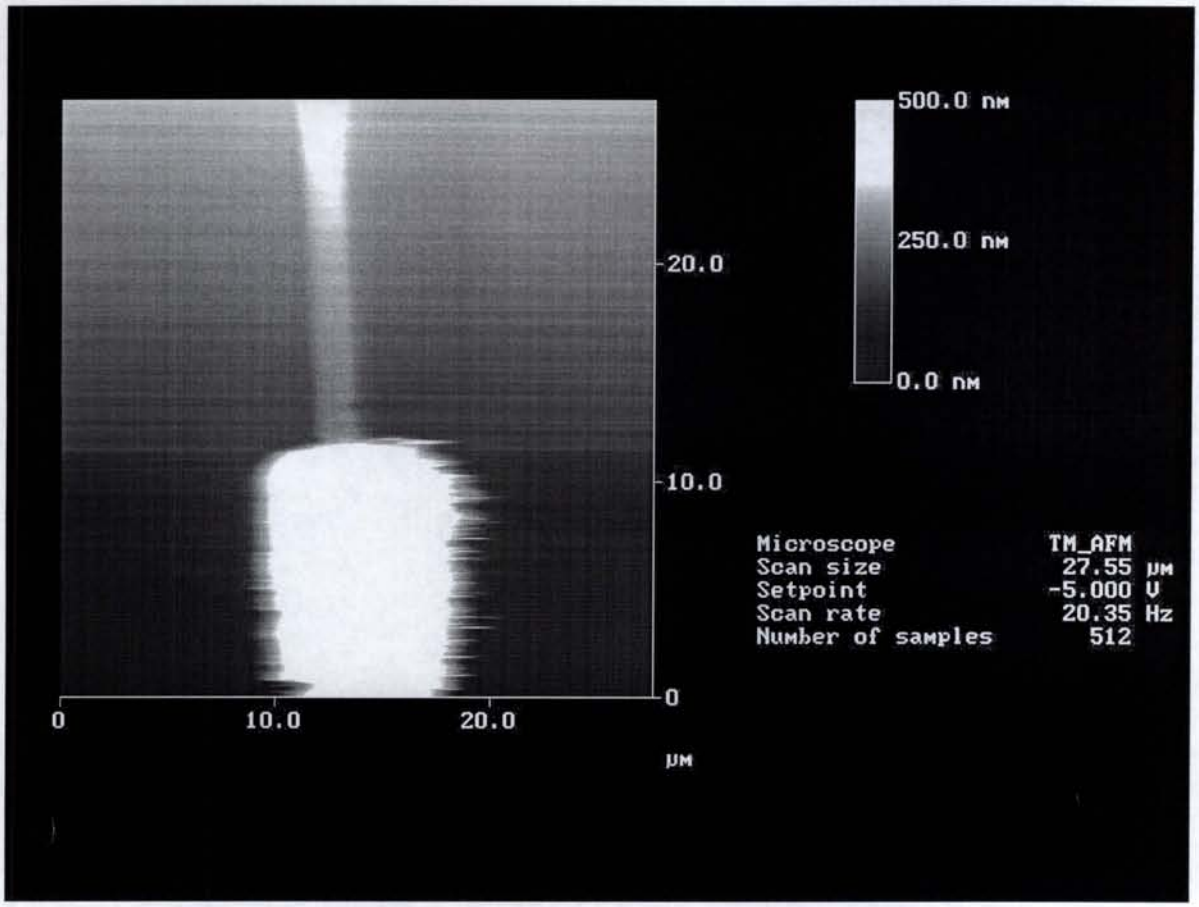

Figure 9: Massive Ni deposition onto device #2 (20,000 100 microsecond pulses at -1.5V) Time = 0 seconds

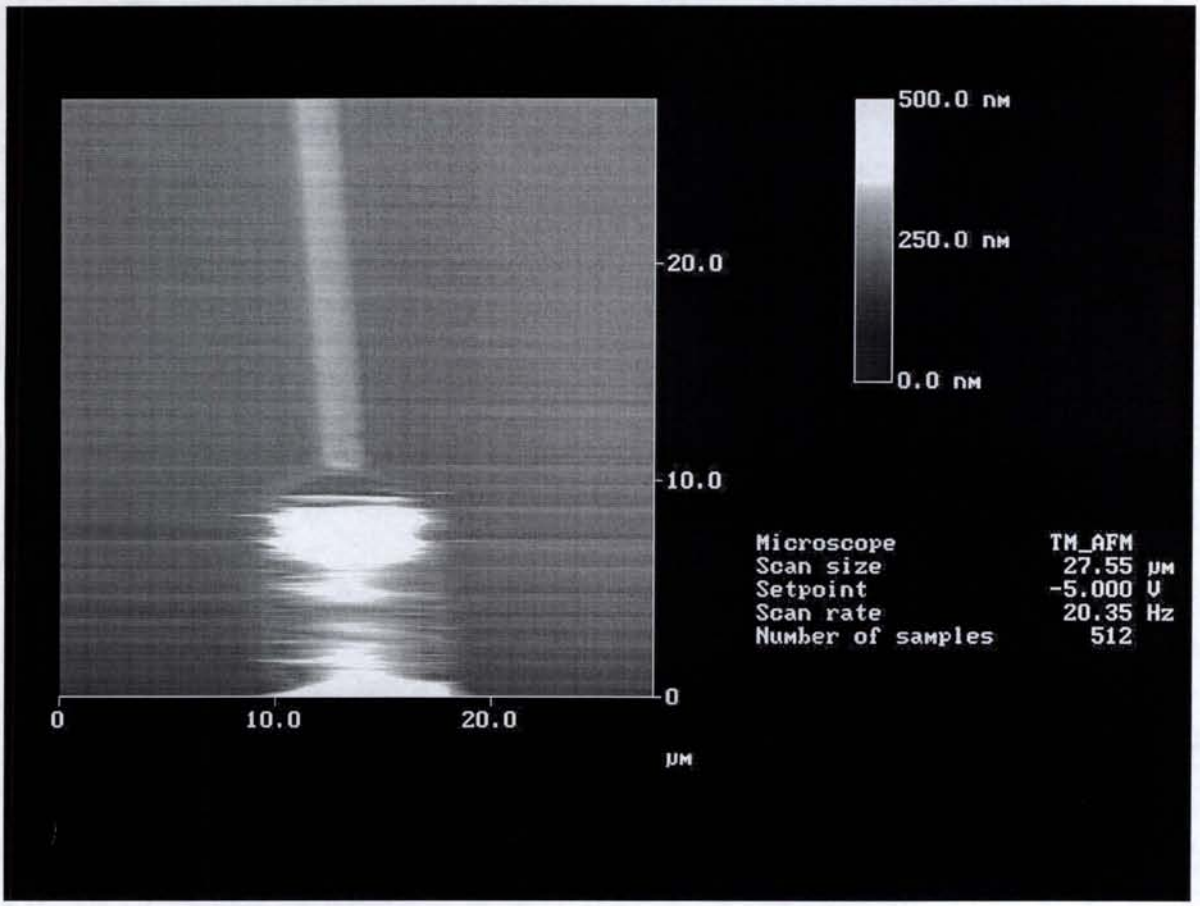

Figure 10: Device 2 at Time = 10 seconds

Tables

	Ground Electrode Depletion			
	Device 4			
	Negative Electrode Height			
	pre-deposition (nm)	post-deposition (nm)	Difference (nm)	% Diff
	68.114	82.66	14.546	21%
	72.431	74.748	2.317	3%
	66.046	84.507	18.461	28%
	69.331	84.098	14.767	21%
	67.388	83.417	16.029	24%
	70.904	90.21	19.306	27%
	67.974	92.18	24.206	36%
	70.827	82.417	11.59	16%
	67.509	83.419	15.91	24%
	70.657	86.523	15.866	22%
STDEV	2.0230904	4.725118704	5.67407	8%
MEAN	69.1181	84.4179	15.2998	22%
95% Conf.	1.253899523	2.928600763	3.516755	5%
	Ground Electrode Height			
	pre-deposition (nm)	post-deposition (nm)	Difference (nm)	% Diff
	67.112	25.51	-41.602	-62%
	67.897	23.076	-44.821	-66%
	67.65	17.79	-49.86	-74%
	68.236	25.51	-42.726	-63%
	68.653	26.183	-42.47	-62%
	67.481	25.843	-41.638	-62%
	67.388	23.833	-43.555	-65%
	68.653	25.093	-43.56	-63%
	72.193	21.399	-50.794	-70%
	65.954	24.258	-41.696	-63%
STDEV	1.636165168	2.581300587	3.356993	4%
MEAN	68.1217	23.8495	-44.2722	-65%
95% Conf.	1.014085541	1.599874912	2.080644	3%

Table 1: Change in height of ground and negative electrodes (deposition on negative, depletion on ground) for device #4

	Ground Electrode Depletion			
	Device 6			
	Negative Electrode Height			
	pre-deposition (nm)	post-deposition (nm)	Difference (nm)	% Diff
	54.966	96.425	41.459	75%
	57.773	102.113	44.34	77%
	62.092	80.733	18.641	30%
	62.186	88.116	25.93	42%
	53.284	88.284	35	66%
	58.673	81.574	22.901	39%
	58.004	83.587	25.583	44%
	60.428	86.945	26.517	44%
	64.118	87.951	23.833	37%
	58.33	90.717	32.387	56%
STDEV	3.332353563	6.567365043	8.380801943	17%
MEAN	58.9854	88.6445	29.6591	51%
95% Conf.	2.065373126	4.070414202	5.19437172	10%
	Ground Electrode Height			
	pre-deposition (nm)	post-deposition (nm)	Difference (nm)	% Diff
	54.803	23.917	-30.886	-56%
	59.831	33.905	-25.926	-43%
	60.265	25.26	-35.005	-58%
	55.291	23.247	-32.044	-58%
	56.648	22.991	-33.657	-59%
	64.027	25.344	-38.683	-60%
	52.126	27.861	-24.265	-47%
	47.839	20.726	-27.113	-57%
	62.684	28.716	-33.968	-54%
	55.978	25.344	-30.634	-55%
STDEV	4.909528599	3.693857618	4.446132763	6%
MEAN	56.9492	25.7311	-31.2181	-55%
95% Conf.	3.042896931	2.289431211	2.755686919	3%

Table 2: Change in height of ground and negative electrodes (deposition on negative, depletion on ground) for device #6

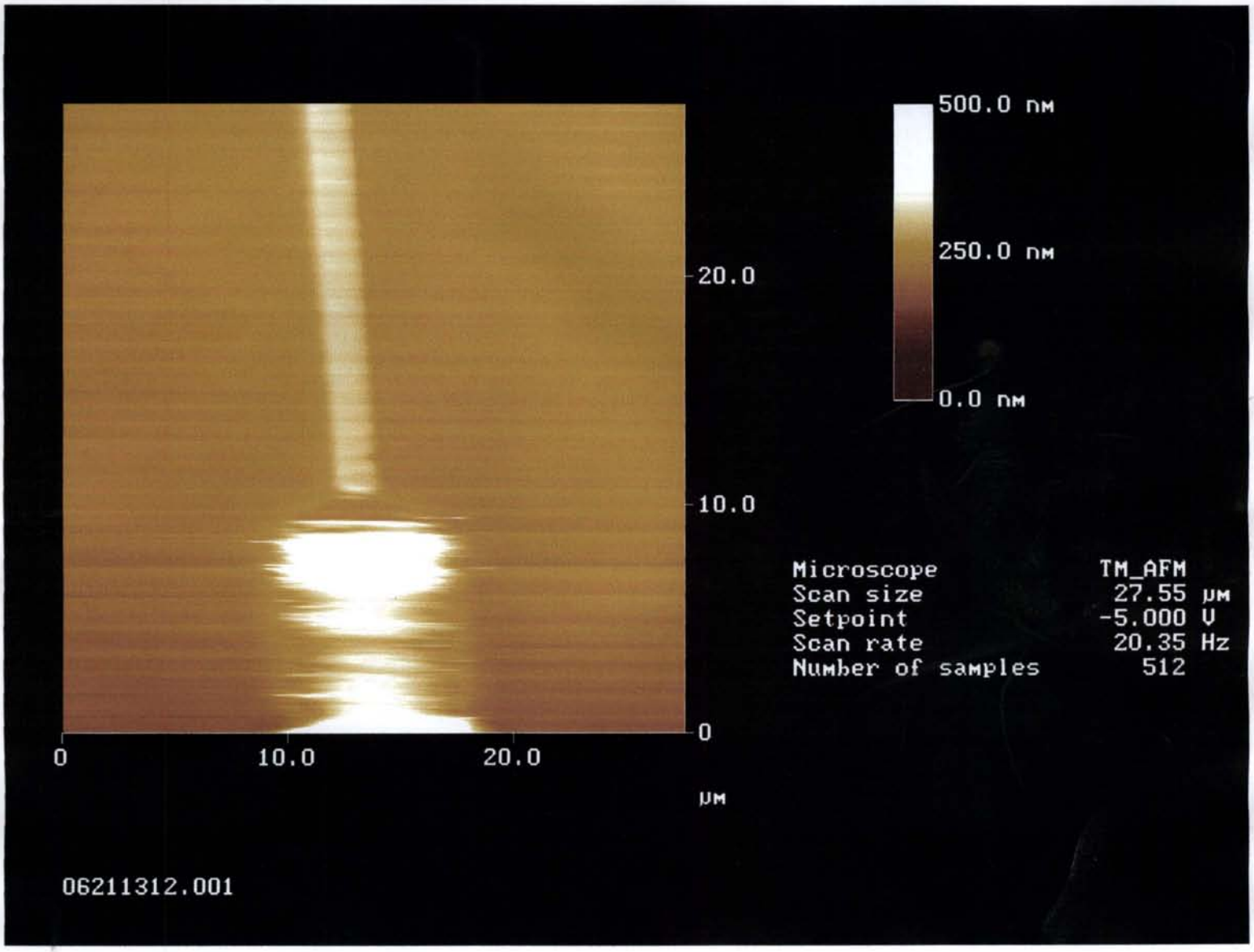
500.0 nm
250.0 nm
0.0 nm
20.0
10.0
0
0
10.0
20.0
µm
Microscope TM_AFM
Scan size 27.55 µm
Setpoint -5.000 V
Scan rate 20.35 Hz
Number of samples 512
06211312.001

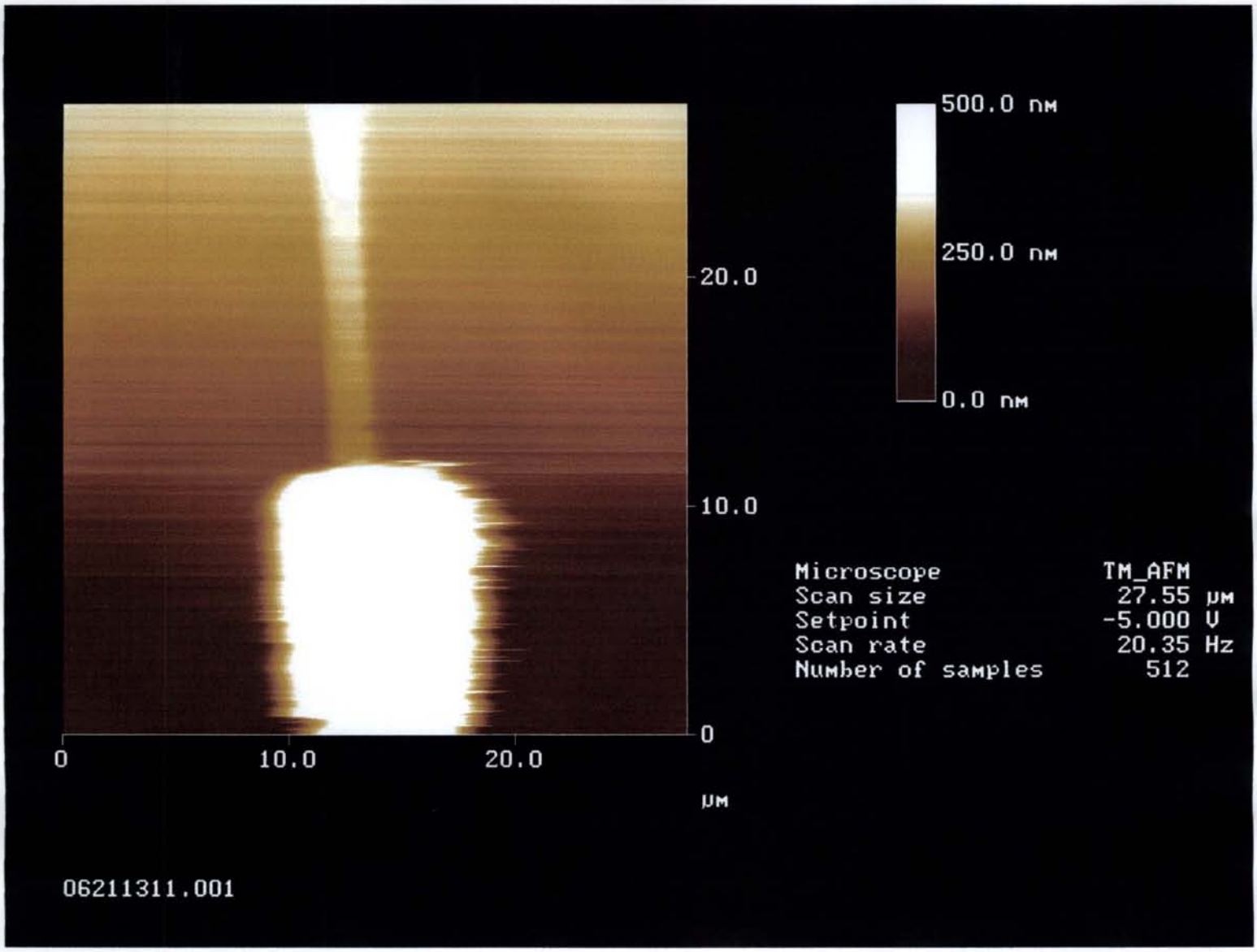
500.0 nm
250.0 nm
0.0 nm
20.0
10.0
0
0
10.0
20.0
µm
Microscope TM_AFM
Scan size 27.55 µm
Setpoint -5.000 V
Scan rate 20.35 Hz
Number of samples 512
06211311.001

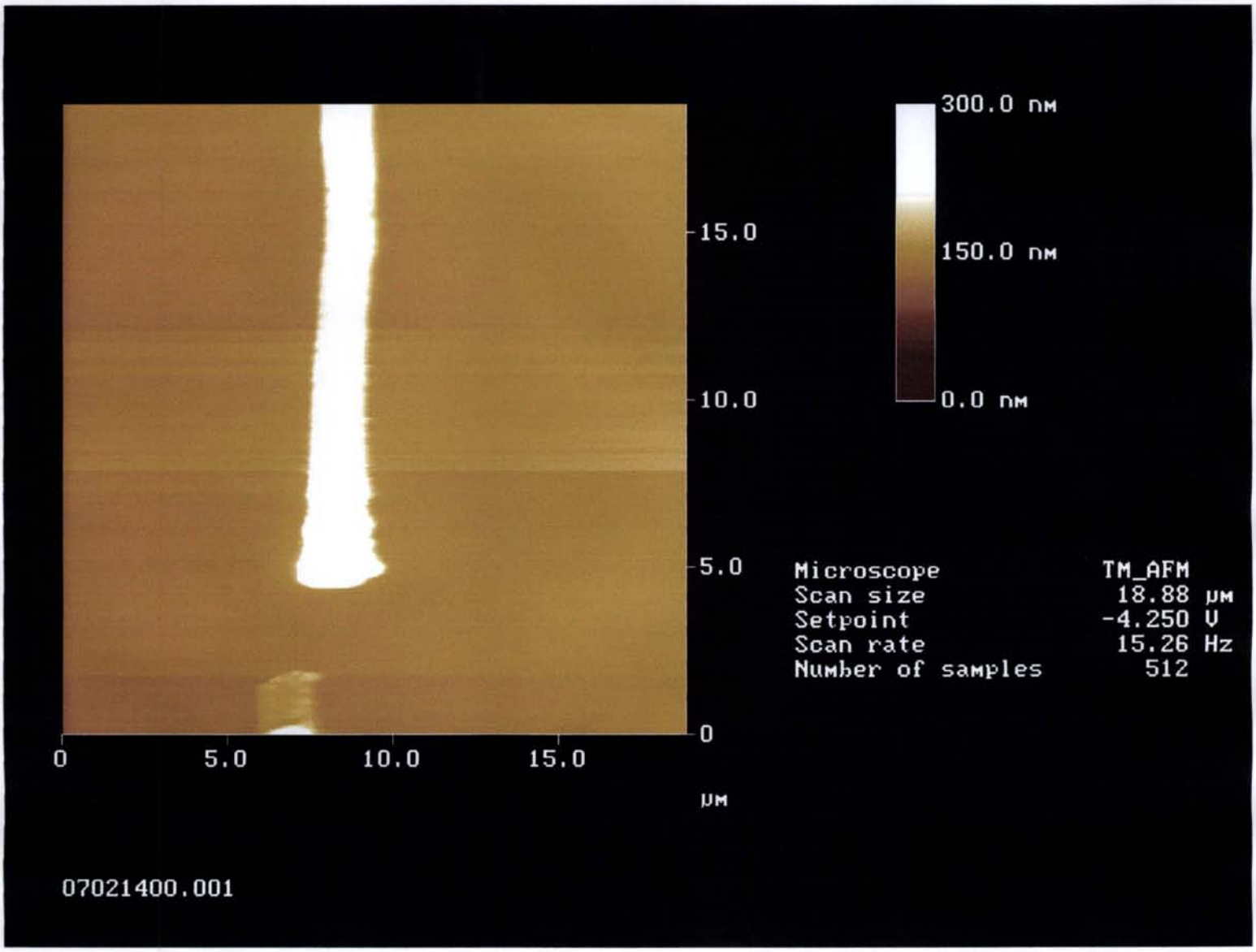
300.0 nm
150.0 nm
0.0 nm
15.0
10.0
5.0
0
0
5.0
10.0
15.0
µm
Microscope TM_AFM
Scan size 18.88 µm
Setpoint -4.250 V
Scan rate 15.26 Hz
Number of samples 512
07021400.001

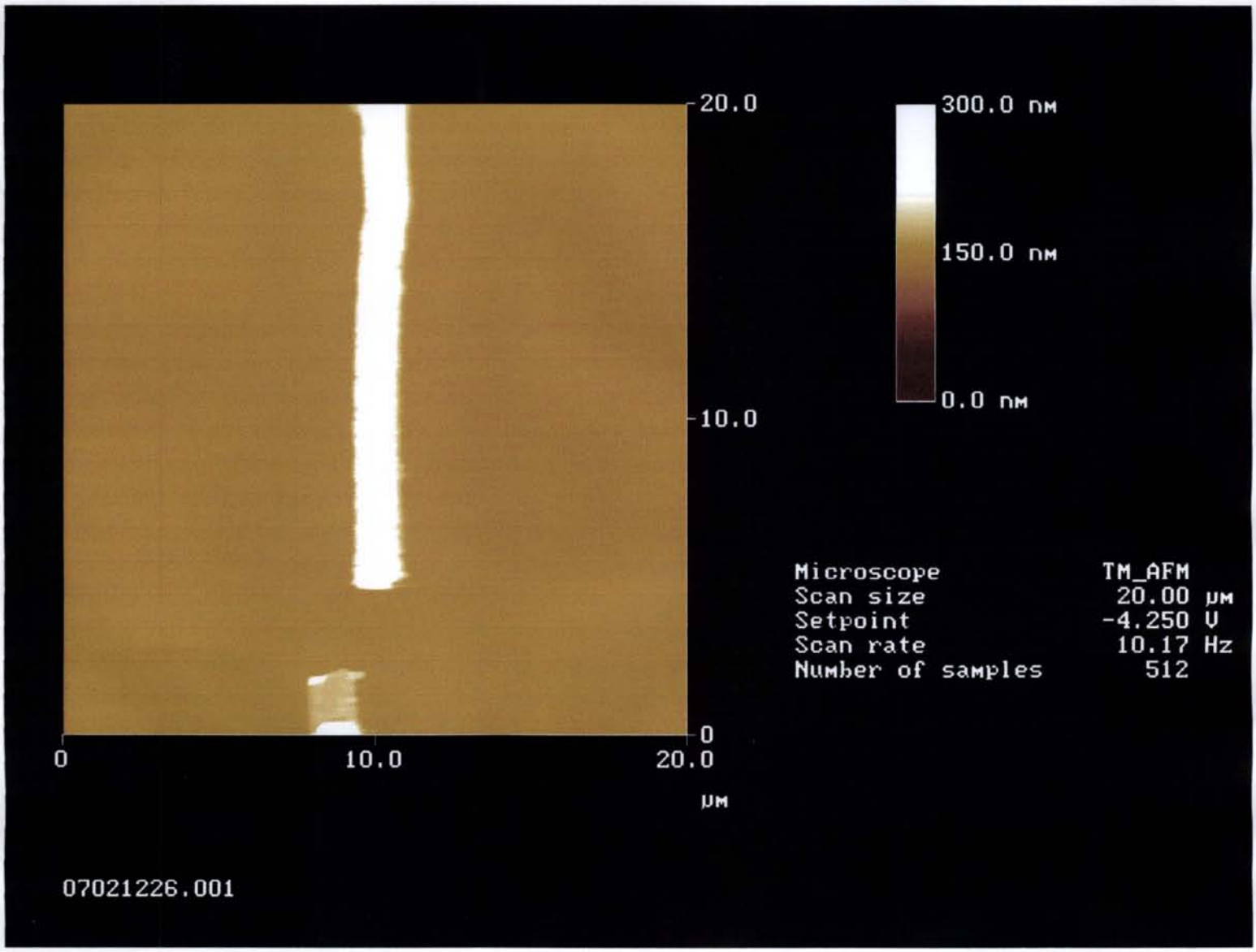
20.0
10.0
0
0
10.0
20.0
µm
300.0 nm
150.0 nm
0.0 nm
Microscope TM_AFM
Scan size 20.00 µm
Setpoint -4.250 V
Scan rate 10.17 Hz
Number of samples 512
07021226.001

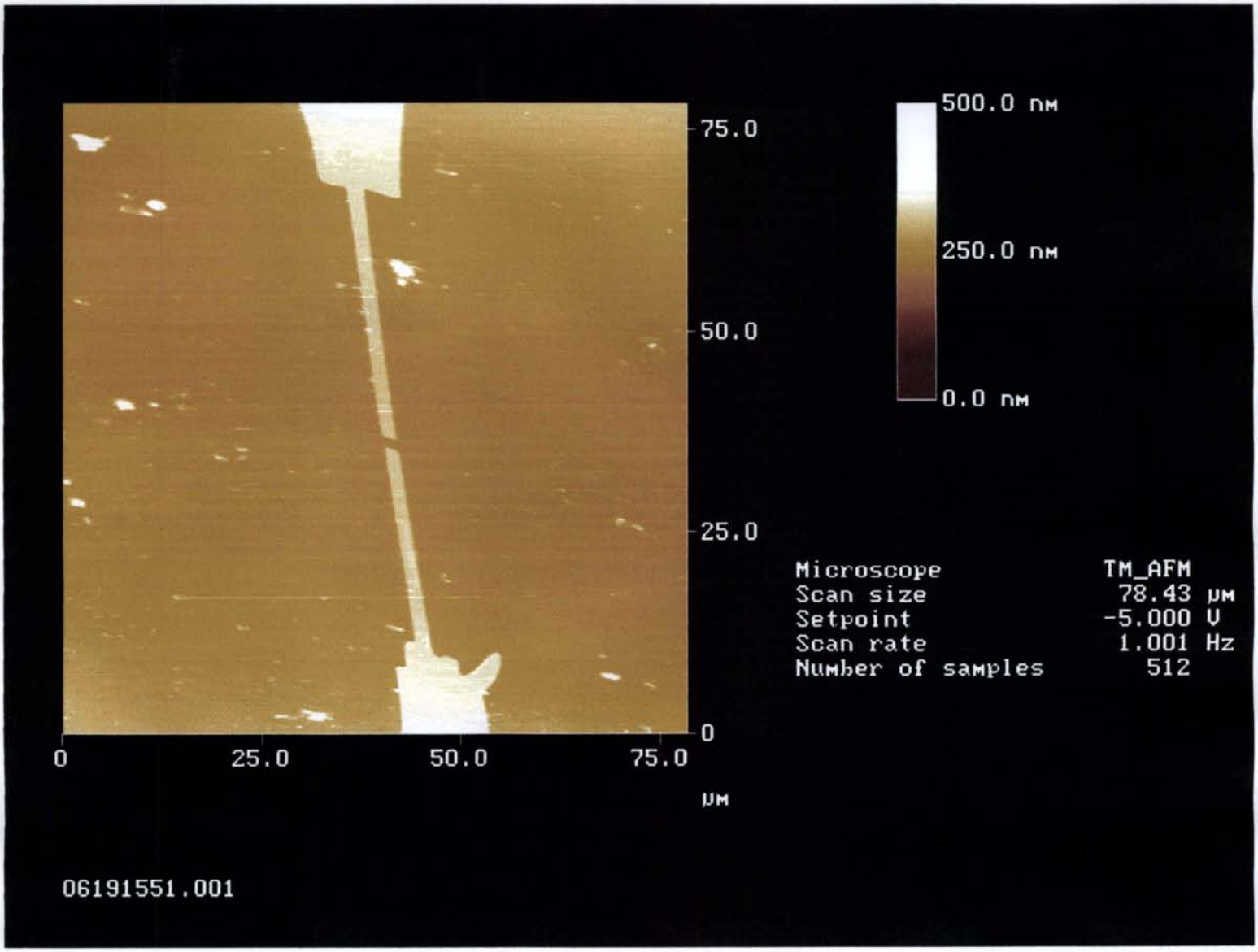
500.0 nm
250.0 nm
0.0 nm
75.0
50.0
25.0
0
0
25.0
50.0
75.0
µm
Microscope TM_AFM
Scan size 78.43 µm
Setpoint -5.000 V
Scan rate 1.001 Hz
Number of samples 512
06191551.001

TMAFM Images

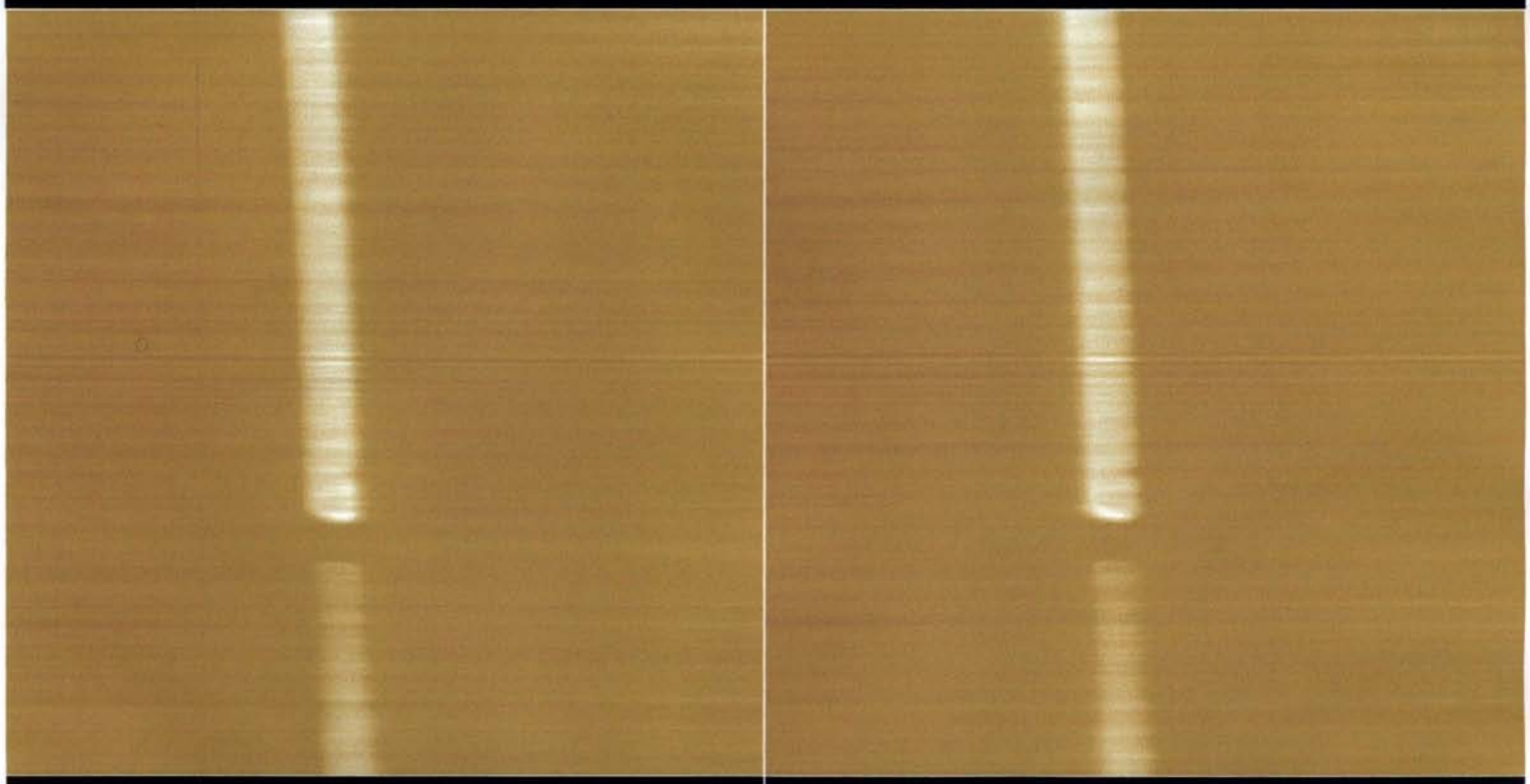

06211312.002

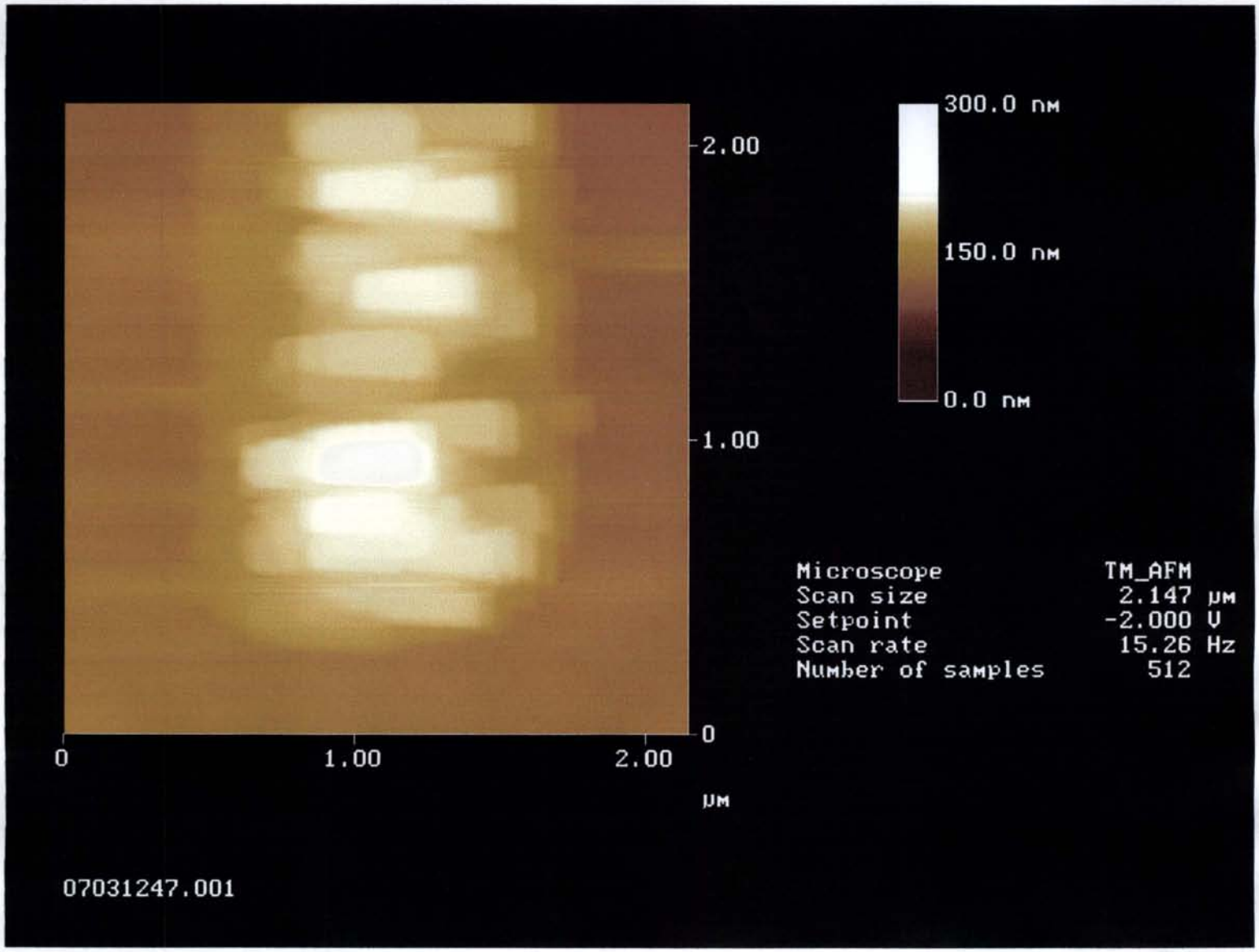
300.0 nm
150.0 nm
0.0 nm
2.00
1.00
0
0
1.00
2.00
µm
Microscope TM_AFM
Scan size 2.147 µm
Setpoint -2.000 V
Scan rate 15.26 Hz
Number of samples 512
07031247.001

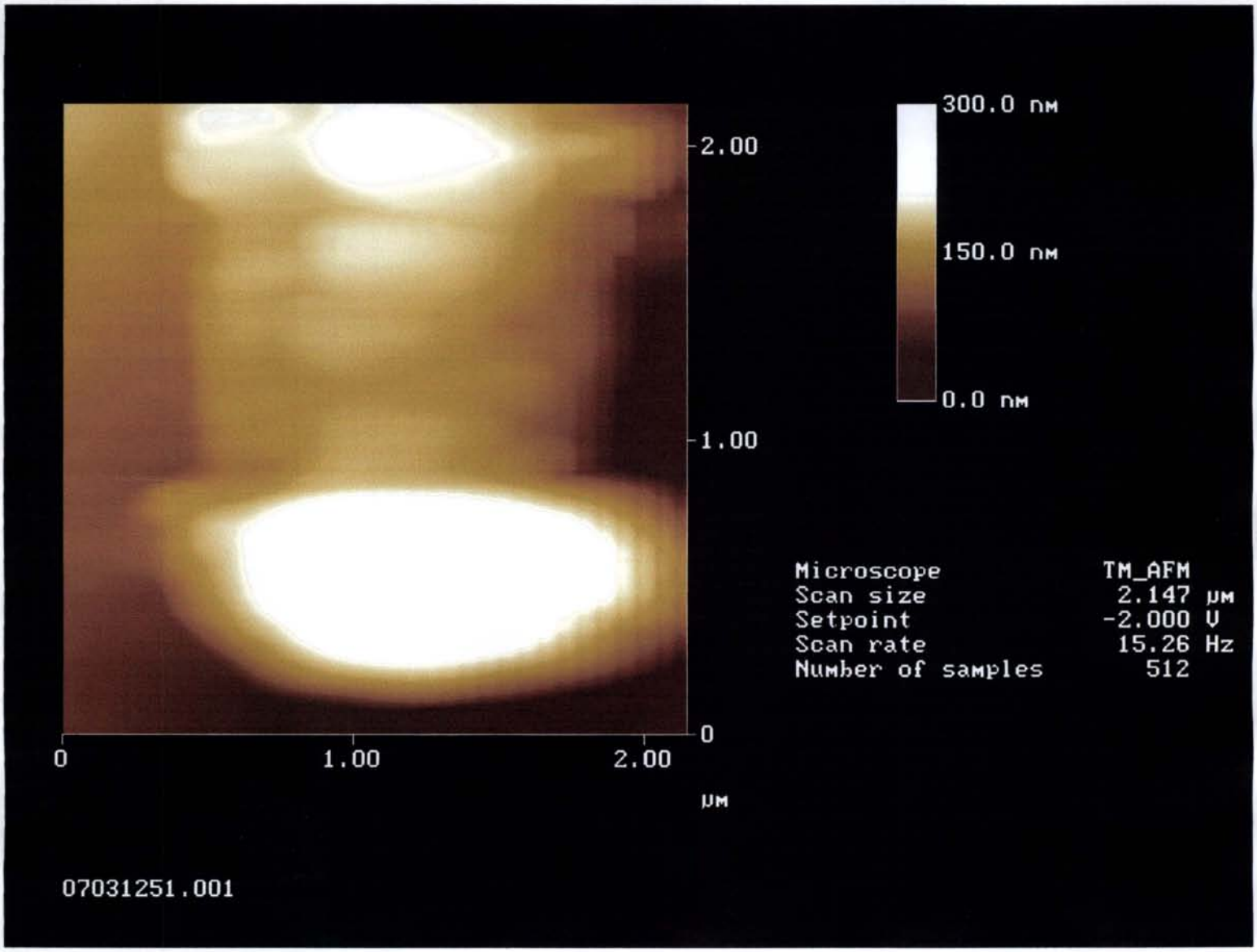
300.0 nm
150.0 nm
0.0 nm
2.00
1.00
0
0
1.00
2.00
µm
Microscope TM_AFM
Scan size 2.147 µm
Setpoint -2.000 V
Scan rate 15.26 Hz
Number of samples 512
07031251.001

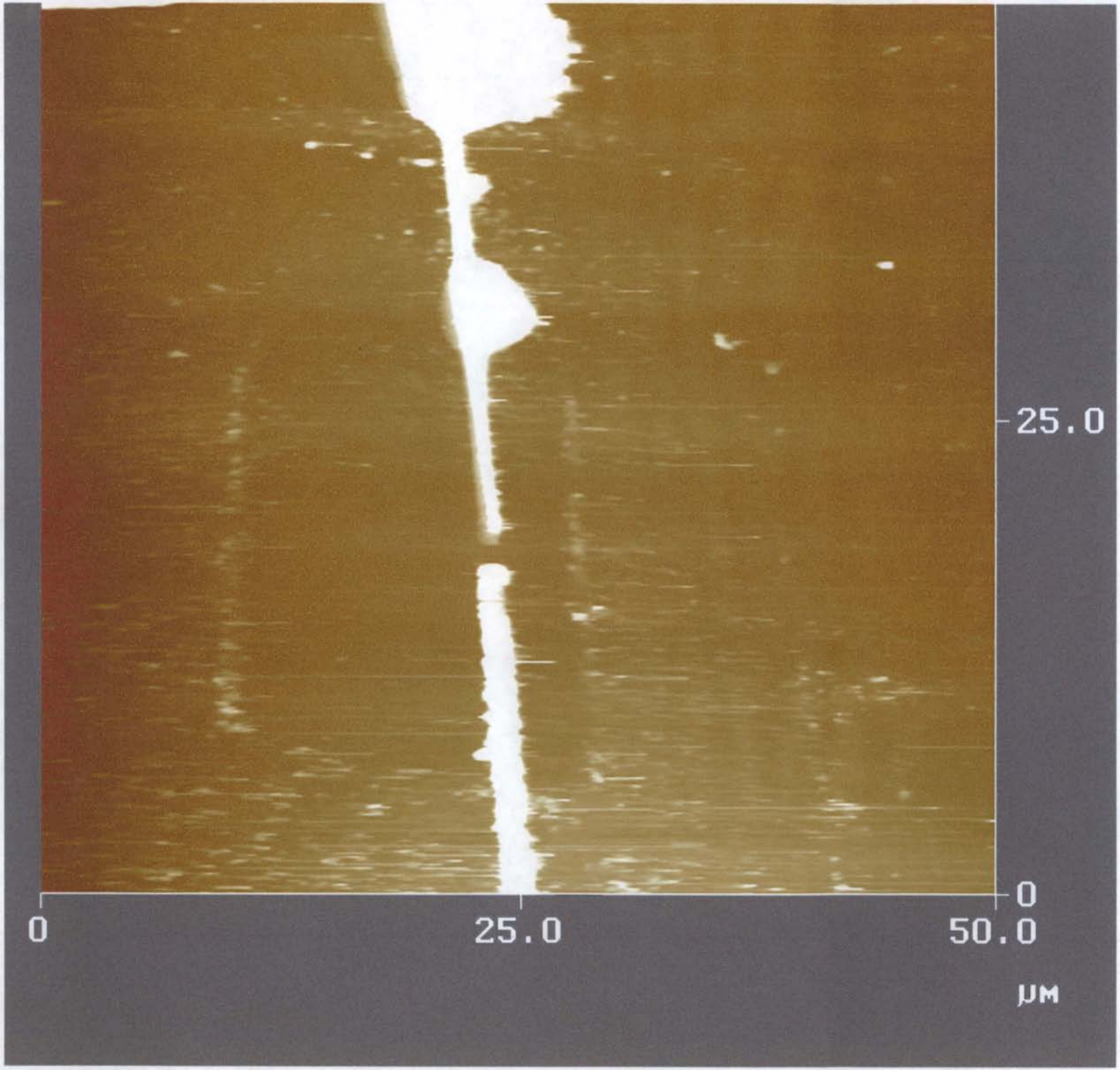

3

0
10.0
20.0
0
10.0
20.0
μm

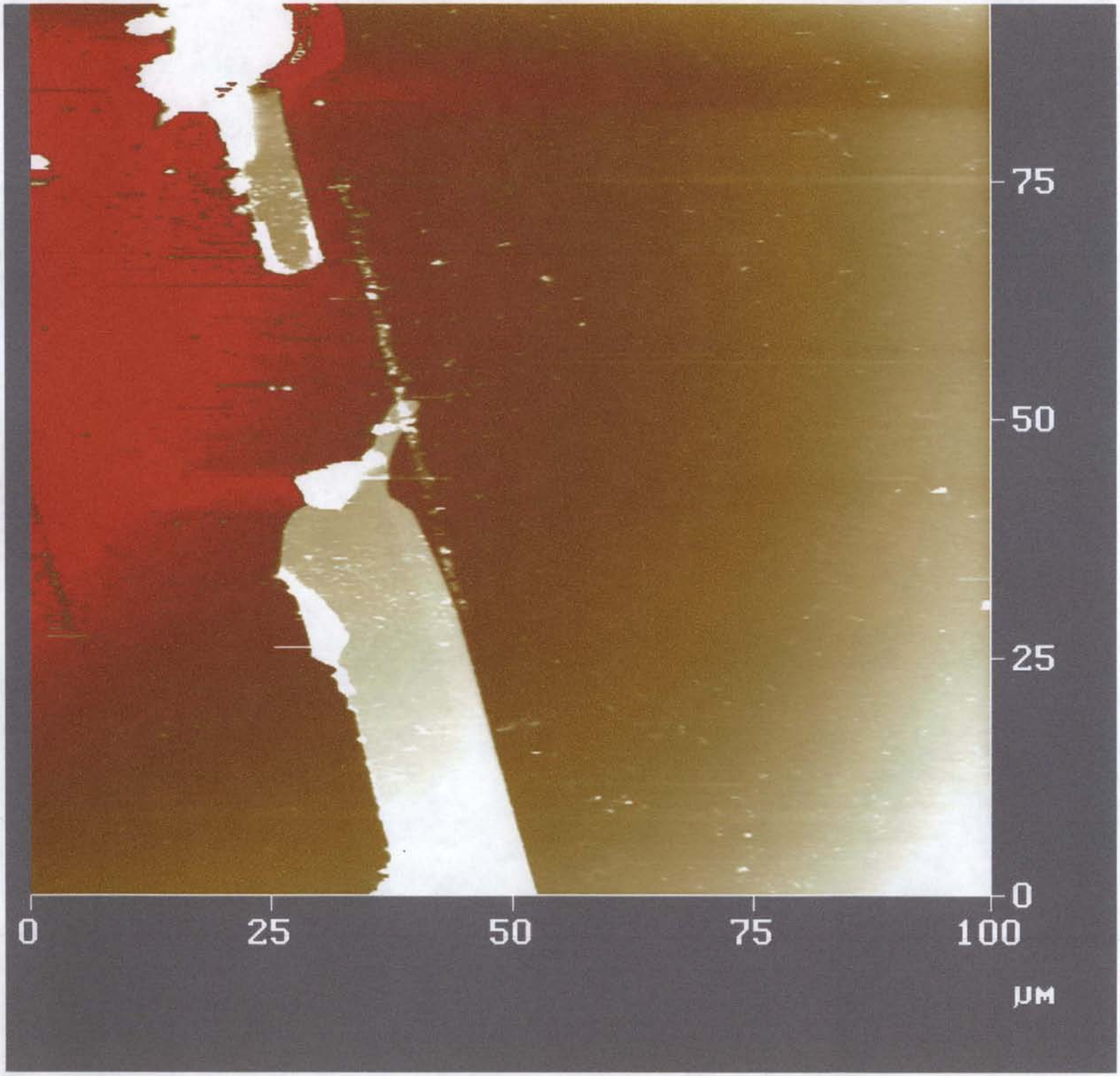
75
50
25
0
0
25
50
75
100
µm

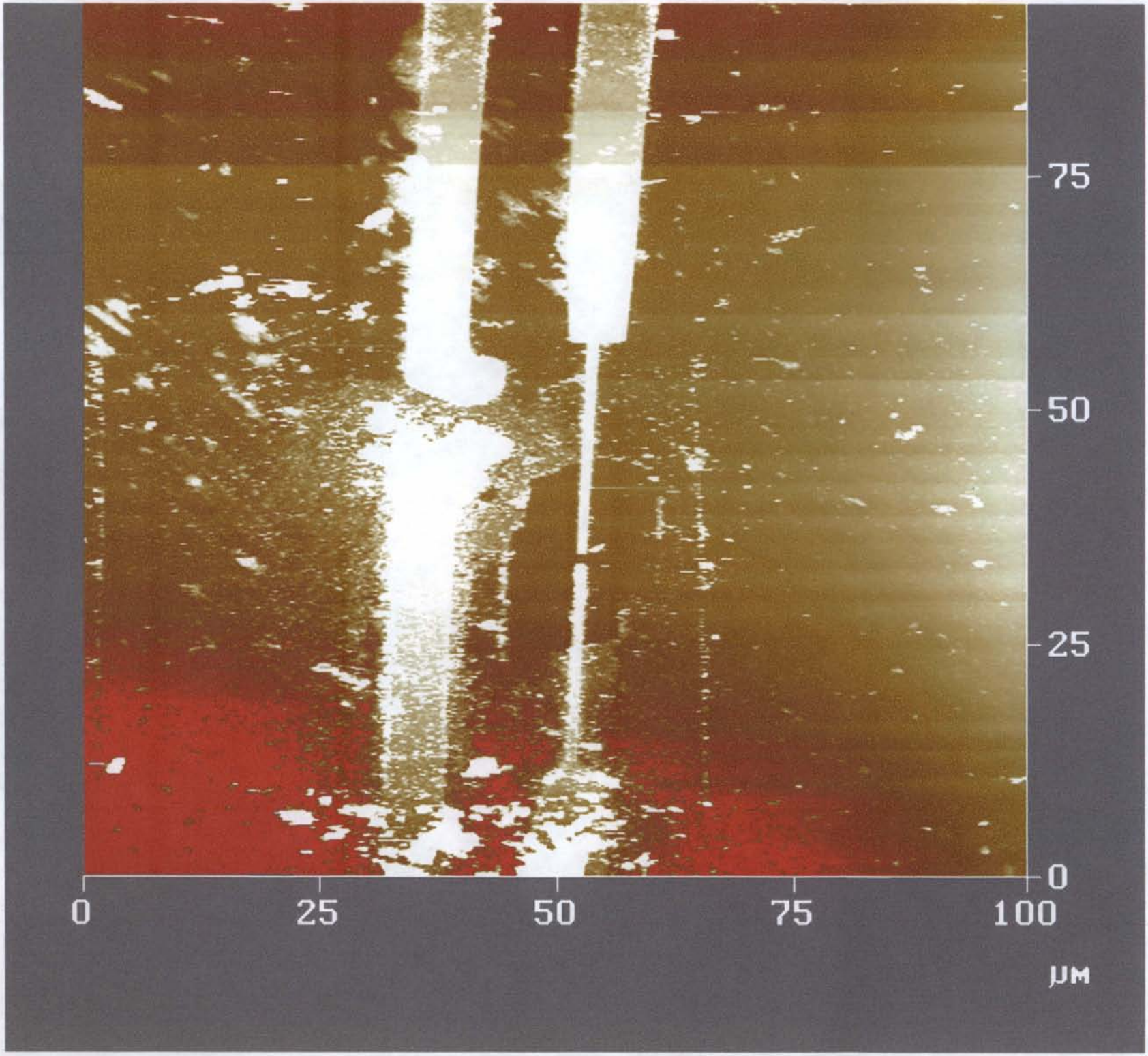
75
50
25
0
0
25
50
75
100
µm

Concept

- A set of gold electrodes is fabricated on a silicon oxide substrate using electron-beam lithography and vapor deposition with an initial distance between electrodes of approximately 1 micron.
- While under a metal-containing electrolyte solution such as $NiCl_2$, a potential is applied between the electrodes, setting up a strongly localized electric field between the tips of the electrodes.
- If a negative potential is used, deposition will occur only on the tip of the negative terminal as electrons are donated to the Pt ion in solution, likewise a positive potential results in depletion at the positive terminal.

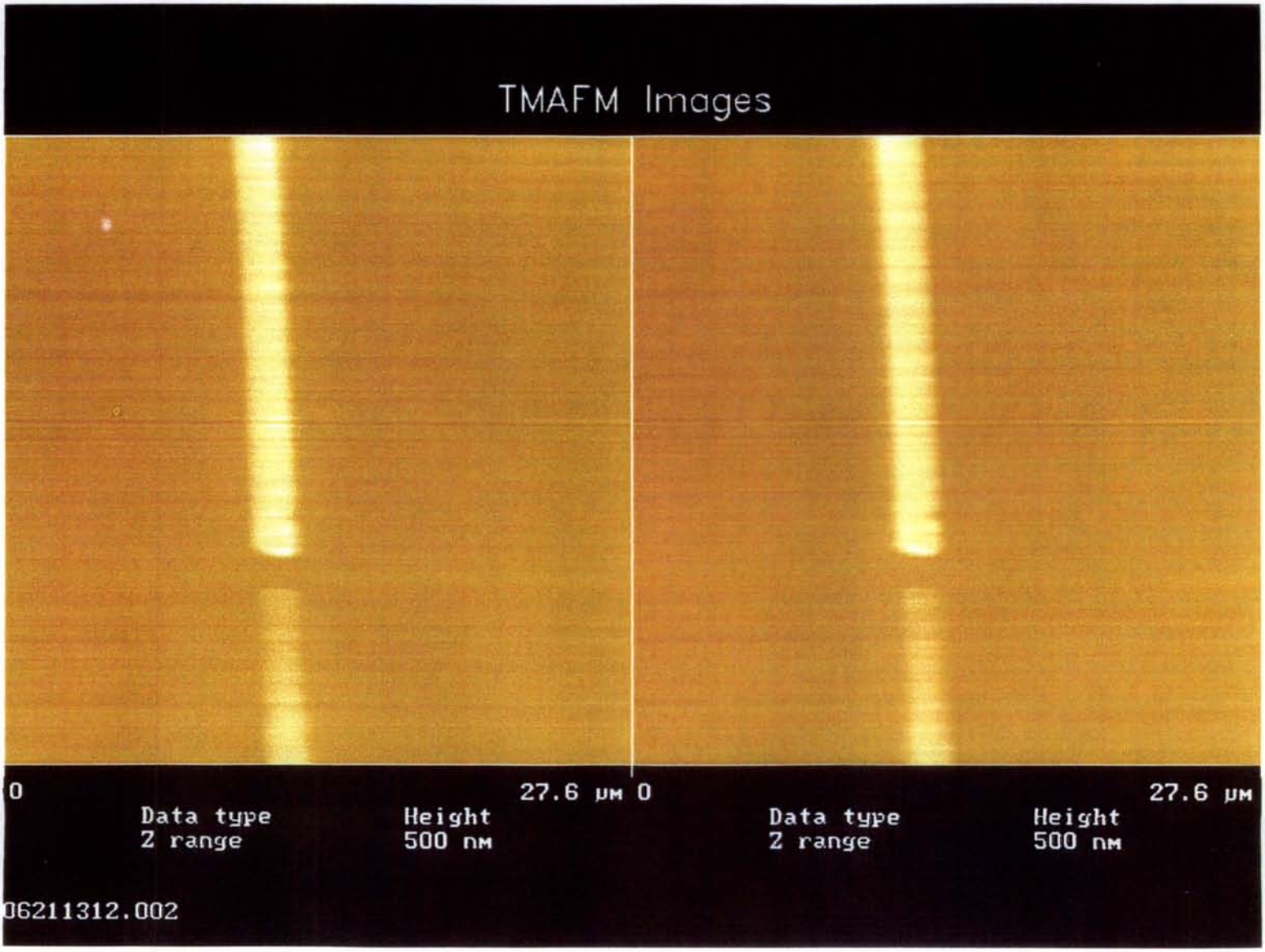
TMAFM Images
0
27.6 µm 0
27.6 µm
Data type
Height
2 range
500 nm
Data type
Height
2 range
500 nm
06211312.002

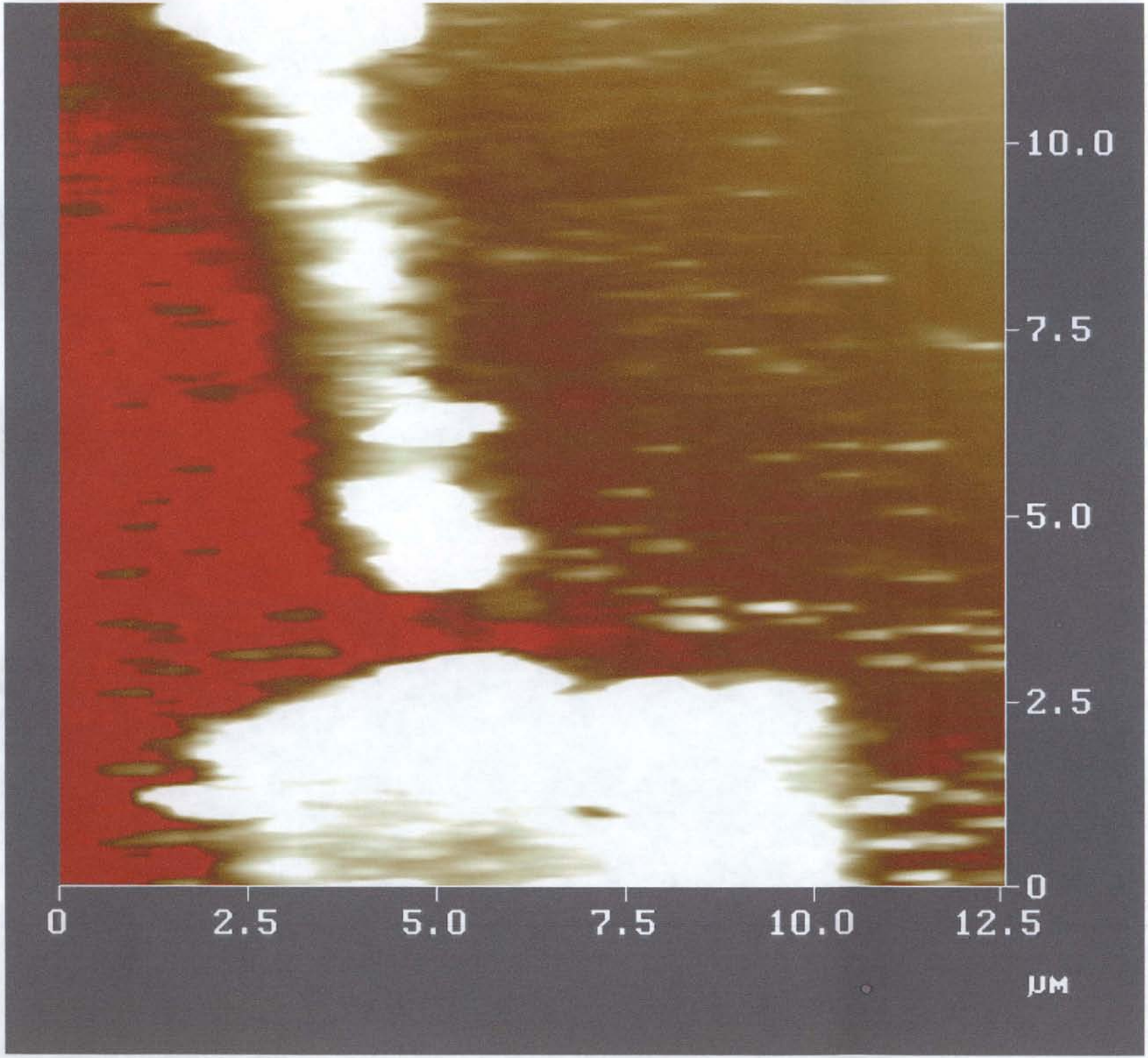

2

Presented to

Kent Wilcher

In Appreciation for Your Contributions as

Energy Research Undergraduate Laboratory Fellowship Participant

Chemical Technology Division
Oak Ridge National Laboratory*

*Managed by UT-Battelle, LLC, for
the U.S. Dept. of Energy under
contract DE-AC05-00OR22725.

7/26/01
Date

L. E. McNeese, Director
Chemical Technology Division

ORNL DWG 2000-374

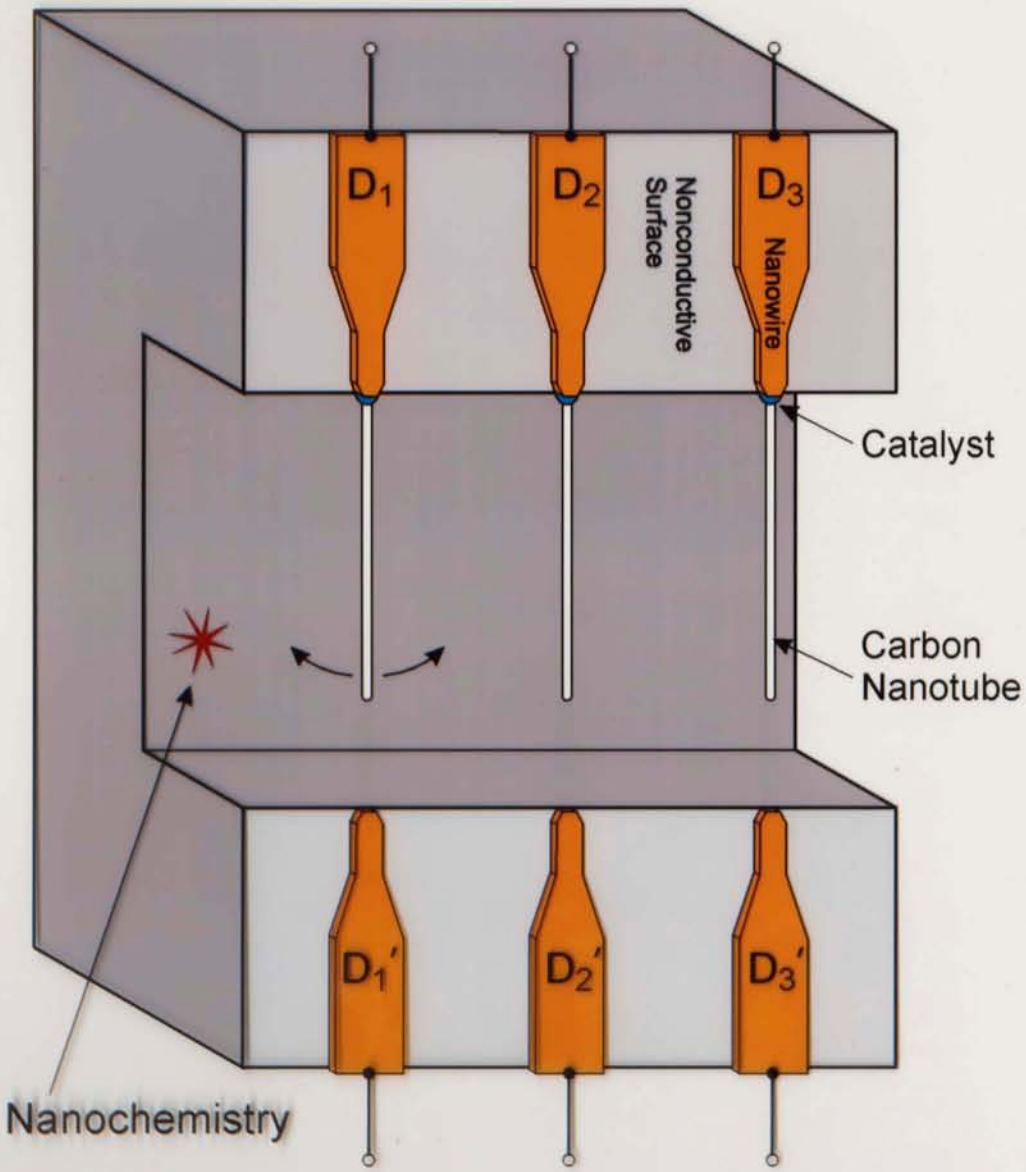

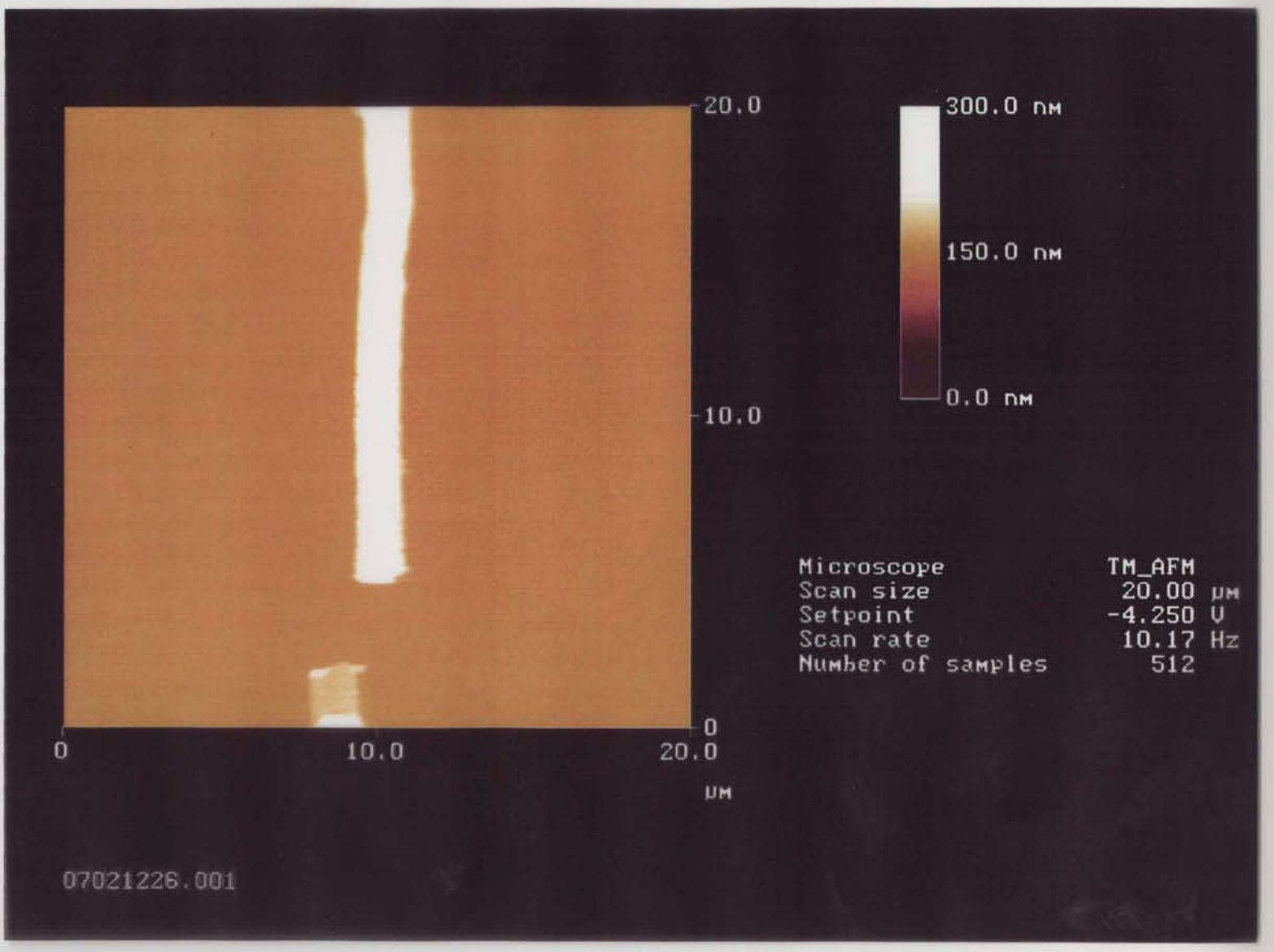
20.0
10.0
0
0
10.0
20.0
µm
300.0 nm
150.0 nm
0.0 nm
Microscope TM_AFM
Scan size 20.00 µm
Setpoint -4.250 V
Scan rate 10.17 Hz
Number of samples 512
07021226.001

Applications

- Controllable nanotube placement at specific sites by deposition of Nickel, a catalyst for nanotube growth.
- DNA sequencing (LDRD proposal already submitted).
- Other molecular applications.

Electrolytic Nanofabrication

Chemical Technology Division

Kent Wilcher

Mentor: Dr. James Lee

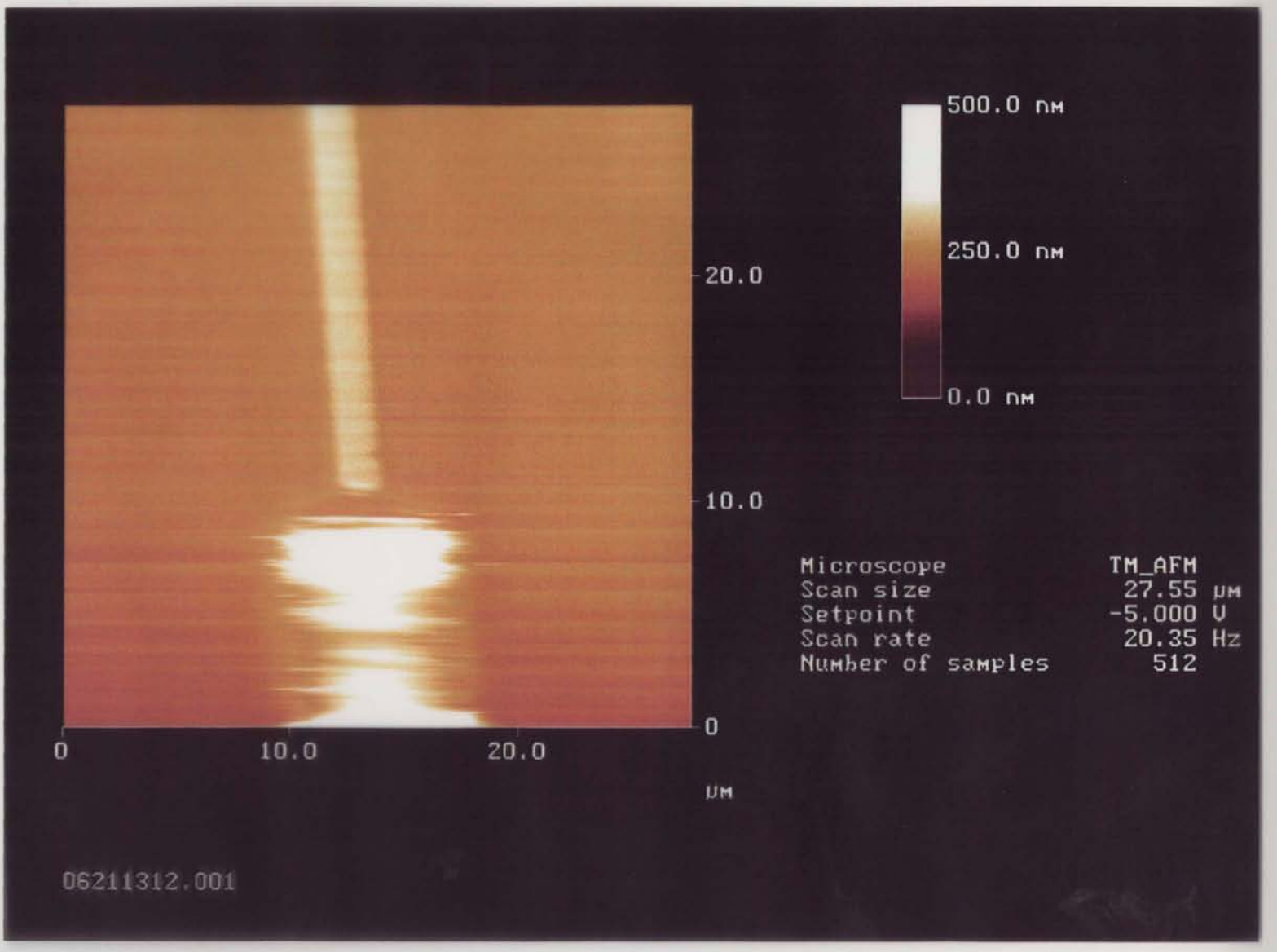
500.0 nm
250.0 nm
0.0 nm
20.0
10.0
0
0
10.0
20.0
µm
Microscope TM_AFM
Scan size 27.55 µm
Setpoint -5.000 V
Scan rate 20.35 Hz
Number of samples 512
06211312.001

Experimental Setup

- An Atomic Force Microscope (AFM) was used to monitor the deposition process in real-time.
- Use of an AFM liquid cell allows scanning while under ionic solutions.
- The programmable voltage source used was capable of changing the duration, magnitude, and time between pulses.

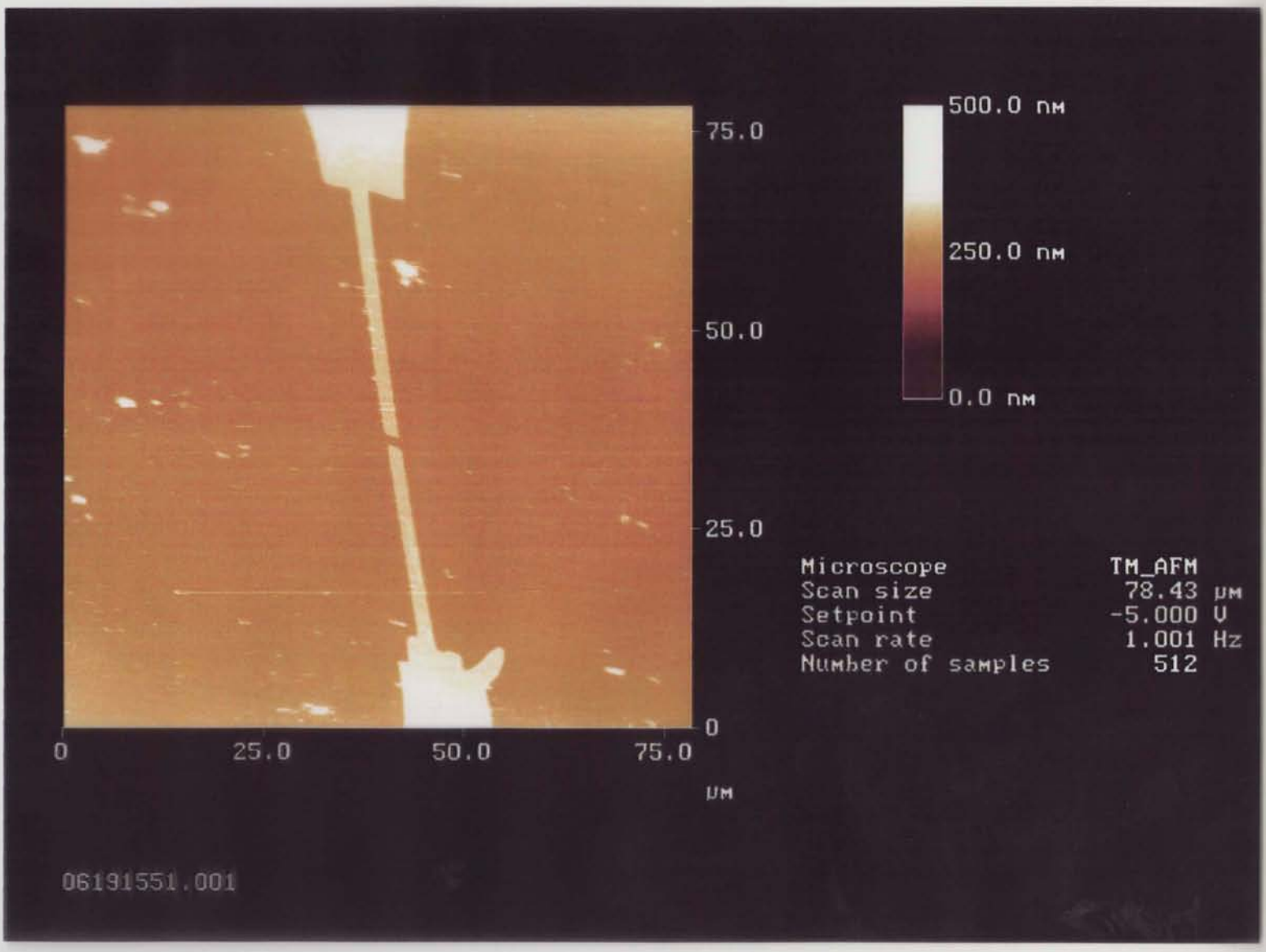
500.0 nm
250.0 nm
0.0 nm
75.0
50.0
25.0
0
0
25.0
50.0
75.0
µm
Microscope TM_AFM
Scan size 78.43 µm
Setpoint -5.000 V
Scan rate 1.001 Hz
Number of samples 512
06191551.001

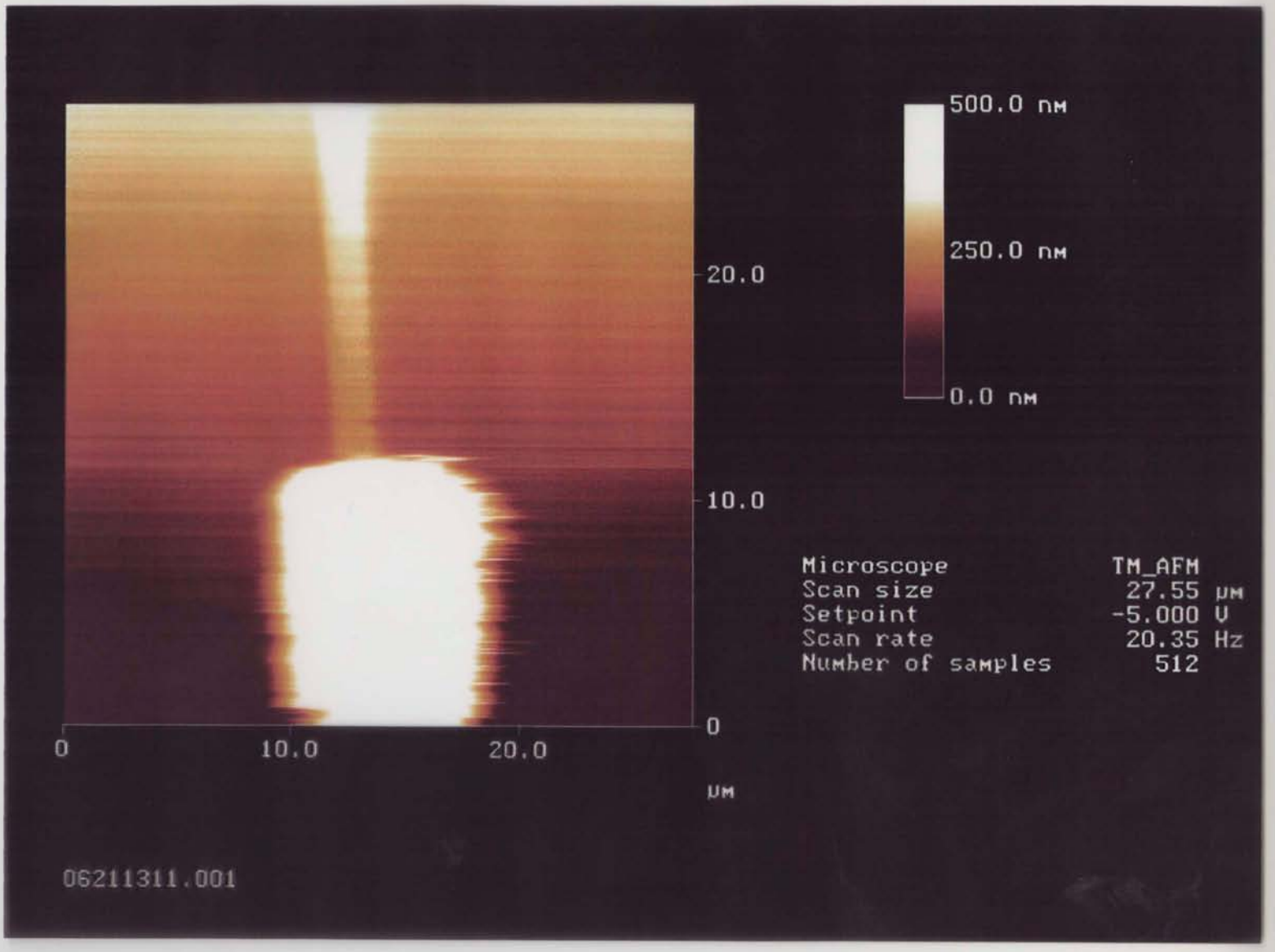
500.0 nm
250.0 nm
0.0 nm
20.0
10.0
0
0
10.0
20.0
µm
Microscope TM_AFM
Scan size 27.55 µm
Setpoint -5.000 V
Scan rate 20.35 Hz
Number of samples 512
06211311.001

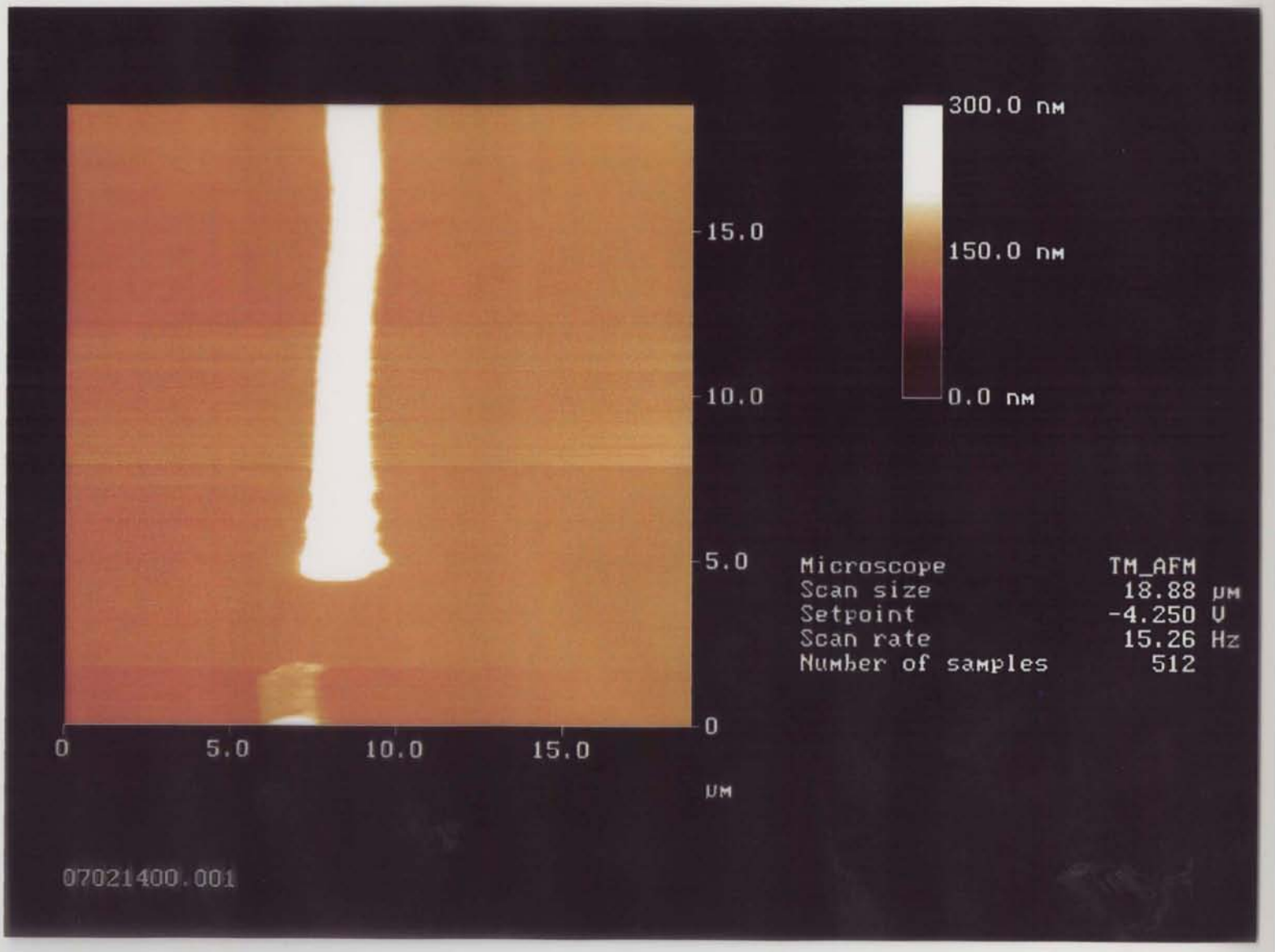
300.0 nm
150.0 nm
0.0 nm
15.0
10.0
5.0
0
0
5.0
10.0
15.0
µm
Microscope TM_AFM
Scan size 18.88 µm
Setpoint -4.250 V
Scan rate 15.26 Hz
Number of samples 512
07021400.001

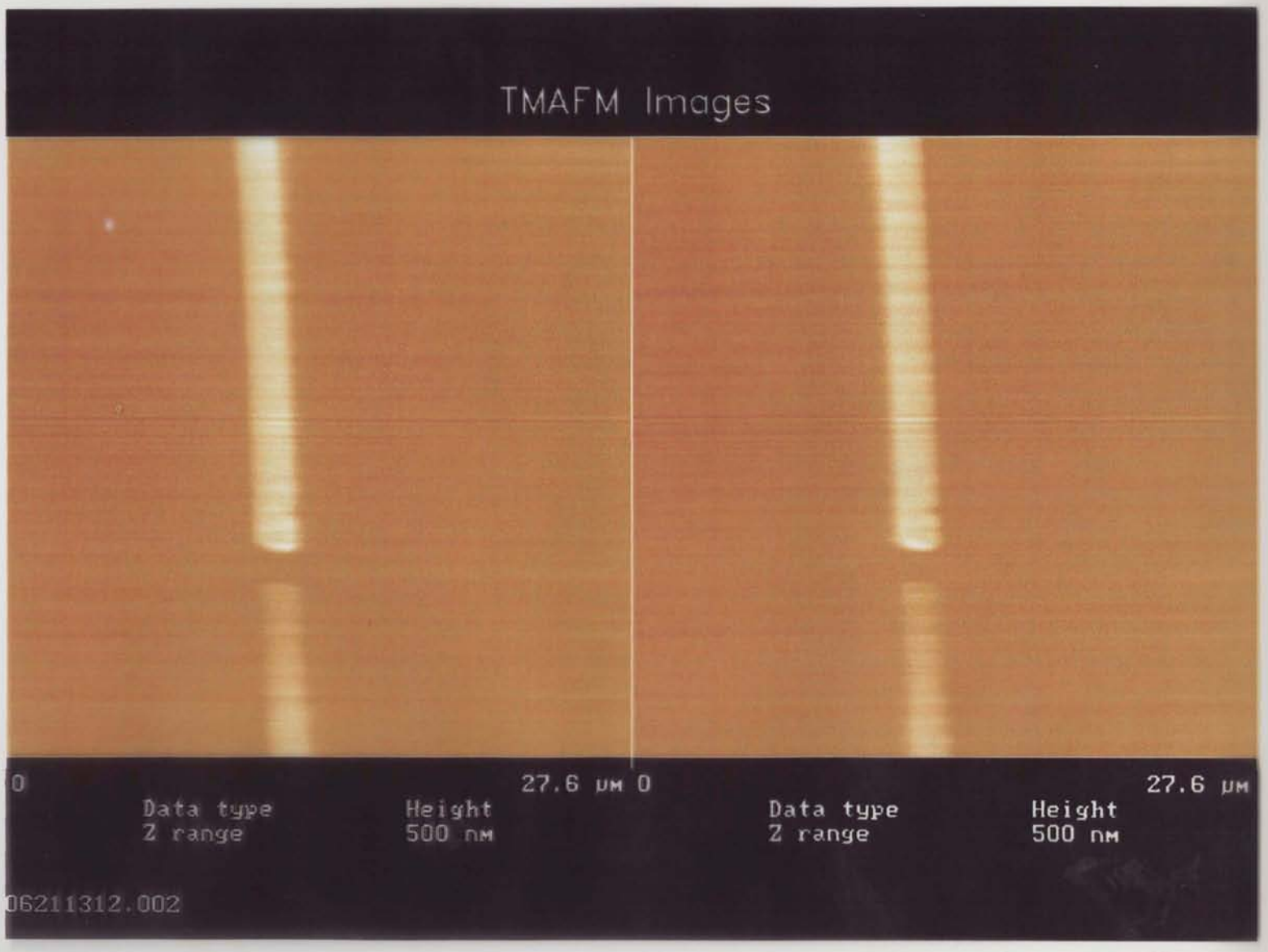
TMAFM Images
0
27.6 µm
Data type
Height
Z range
500 nm
0
27.6 µm
Data type
Height
Z range
500 nm
06211312.002

ORNL DWG 99C-445

Nanometer-Scale Welding Through Electric Field–Directed and Programmable Pulsing Electrolytic Metal (Pt) Deposition with a Bypassing Circuit